COOP-CT-2004-513046

REFLECTS

Novel bifacial single-substrate solar cell utilising reflected solar radiation

Co-operative Research Projects

Integrating and strengthening the ERA

Final Activity Report

Period covered: from	1st November 2004	to	1st November 2006
Date of preparation:	15th December, 2006		
Start date of project:	1st November 2004		
Duration:	24 months		
Project coordinator name:	Henk van Ekelenburg		
Project coordinator organisation name:	Pro Support B.V.		

Table of Contents

Publishable executive summary

Project Objectives

REFLECTS aims at manufacturing mono-crystalline silicium (c-Si) solar cells with an increased efficiency by also making use of the solar radiation reflected from earth surface. Studies indicate that this energy is in the order of 30-50% of direct radiation, and by adopting high-reflective surfaces (mirrors) this could be exploited. The technical route foreseen to utilise the reflected solar radiation is making a double-sided (bifacial) solar cell.

The project proposed here aims to prepare the back end of an c-Si solar cell by applying a recently established Lithuanian technology for producing single-sided solar cells, based on self-formation [2, 3]. In this technology, the + and - conductors are both at the front end, and two-sided processes simply can copy the process to the back-end. This process is far simpler than the manufacturing process of the current two-sided solar cells. Despite foreseen losses in the bulk of the wafer, the expected cell efficiency – based on theoretical calculations – is a whopping 26% (65% higher than commercial single-sided c-Si cells) with only 10-15% cost increase compared to single-sided cells, so the €/W_p ratio is expected to be effectively reduced by ~50% compared to commercially available single-sided c-Si solar cells. Furthermore, a competitive reflector will be developed which is optimised for c-Si bifacial solar cells.

In addition, the REFLECTS project supports following societal and policy objectives:

- Mitigate the environmental effects from the emissions of greenhouse gasses and local pollution caused by the burning of fossil fuels, aiming at a 15% reduction by the year 2010 from the 1990 level;
- Improve the diversity, self-sufficiency and security of EU energy supplies, especially with respect to the dependence on imported energy which is now at 50% and expected to rise to 70% by 2020 if no action is taken;
- Reduce the pressures on governments (taxpayers) and utility companies to provide enough electricity to meet future demands;
- Reduce the cost of energy and dependence on utilities for consumers;
- Attract investors that will back an industry that's largely driven by SMEs that design, manufacture, and distribute renewable energy systems, thus increasing jobs in data acquisition systems, engineering design, manufacturing, and data analysis as well as distribution, marketing, sales and service.

Furthermore, the quality of life for people in under-developed countries will be enhanced by providing access to equipment such at radio/TV, electrical appliances, etc. Other possible benefits outside Europe are reducing the destruction of rain forests and saving threatened species.

Contractors involved

Partic. Role	Partic. no.	Participant name	Participant short name	Country
CR	1	Millennium Electric T.O.U. Ltd.	MILLENNIUM	IL
CR	2	Girasol B.V.	GIRASOL	NL
CR	3	UAB "TELEBALTIKOS" IMPORTAS IR EKSPORTAS	TELEBALTIKA	LT
CR	4	Saules Energija UAB	SAULES ENERGIJA	LT
CR	5	Optical Products Ltd	OP	UK
CR	6	Winsund International Ltd.	WINSUND	UK
CR	7	Badham Farms	BADHAM FARMS	UK
CR	8	Heavens Solar Technology Ltd.	HEAVENS SOLAR	UK
CO	9	Pro Support B.V.	PSU	NL
CR	10	Institute of Lithuanian Scientific Society	MSI	LT
CR	11	Institut für Solarenergieforschung GmbH Hameln / Emmerthal	ISFH	D
CR	12	Centre for Renewable Energy Sources	CRES	EL

Co-ordinator contact details

Pro Support B.V.

Amarilstraat 11

7554 TV Hengelo

Netherlands

tel: 0031 74 2551160

mob +31 653283486

fax: 0031 74 2508171

info@prosupport-nl.com

Work performed

Crystalline-Si bifacial solar cells have been developed on basis of the ORTO-structure that makes use of both horizontal and vertical planes. Based on self-formation, which is largely steered by smart software, simulation runs have been performed. Secondly, a novel reflector has been researched that is able to reflect an maximum amount of albedo sunlight, yet very cheap to manufacture. A prototype has been conceived and tested.

Results achieved so far and expected end results

Figure 1 illustrates the ORTO solar cell cross section. Two groups of rectangular grooves are created in the wafer: for emitter and for base. The emitter is formed by phosphorous diffusion. The boron diffused grooves provide a BSF. The distance between grooves are less than diffusion length of minority charge carriers. In this mode, the photo-generated carriers must be effectively separated by space charge region. The structure is “thick” for photon flow direction and “thin” along emitter-base direction. The metal contacts for emitter and base are formed on the slots walls by the obliquely metal evaporation. Because metal stripes are placed perpendicular to photon direction the shadowing of structure by contacts is minimal. The rear side of structure is free of contacts and effectively passivated by SiN_x. So, the ORTO structure acts as a bifacial solar cell.

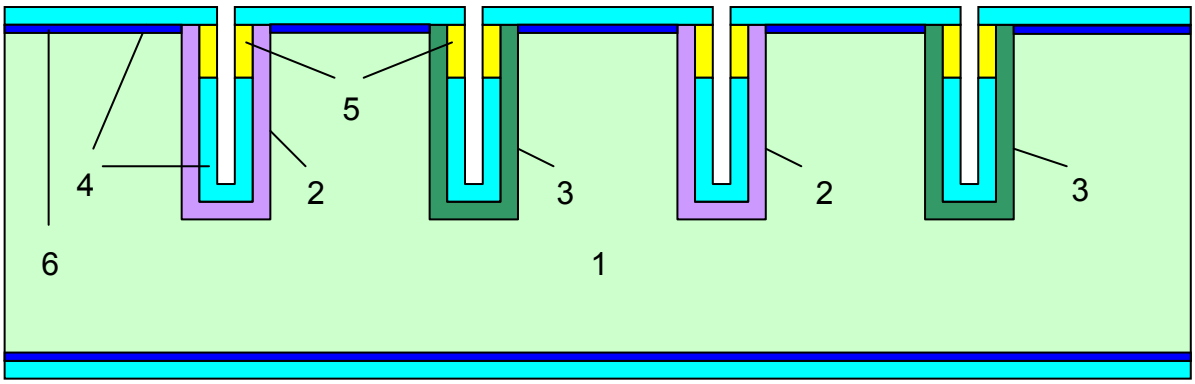

Figure 1: ORTO Solar Cell; Legenda: 1 – Si, p-type; 2 – Emitter, n^+; 3 – BSF, p^+; 4 – ARC, SiN_x; 5 – Al

Impact

The use of renewable energies, and in particular photovoltaics (PV), is one of the most attractive solutions to overcome the problems caused by conventional energy sources. Whilst much achievements have been made over the last couple of decades to reduce the costs of PV cells, their costs are presently still the main obstacle for a world-wide increased utilisation of electric power provided by this clean and renewable technology. Therefore, the need for innovative, competitive manufacturing concepts is compelling.

Plans have been drawn up to commercially exploit the bifacial solar system developed identifying possible markets, pricing and distribution, and will continuously updated.

Main publishable results

Experimental modules have been manufactured with a number of different cell structures, and evaluated in laboratory conditions. Following interesting results were achieved so far.

Illumination	V_{OC} [mV]	J_{SC} [mA/cm^2]	FF [%]	Efficiency [%]
Unmetalised FS	639	34.3	77.6	17.0
OECO-metalised RS	635	33.2	76.9	16.2

SECTION 1 Project objectives and major achievements during the reporting period

1.1 Overview of general project objectives in relation to the state-of-the-art

Objective	Milestone/Deliverable	Month for delivery
To develop mono-crystalline silicium (c-Si) bifacial solar cells with an increased efficiency	Functional and technical specifications for reflector, solar cell and associated self-formation technology defined	3
	Reflector prototype developed	9
	Optimal solar cell ORTO structure defined	12
	Production protocol (routing card) of bifacial c-Si solar cells manufacturing	15
	Software program for optimisation of self-formation technology developed	16
To test, validate system in laboratory and perform integrated system field evaluation	Solar cell + module performance evaluated	22
	Economical evaluation performed	22
	Field tests accomplished	24
To prepare conditions for REFLECTS introduction to market	Completion of the Plan for using and disseminating knowledge	24
	Future exploitation plans established	24
	Website and other dissemination materials prepared	24

1.2 Summary of recommendations from previous reviews (if any) and follow-up by the consortium

[intentionally left blank – no such remarks received]

1.3 Summary of the objectives for the reporting period, work performed, contractors involved and the main achievements in the period

Objective	Milestone/Deliverable	Month for delivery
To develop mono-crystalline silicium (c-Si) bifacial solar cells with an increased efficiency	Production protocol (routing card) of bifacial c-Si solar cells manufacturing	15
	Software program for optimisation of self-formation technology developed	16
To test, validate system in laboratory and perform integrated system field evaluation	Solar cell + module performance evaluated	22
	Economical evaluation performed	22
To prepare conditions for REFLECTS introduction to market	Completion of the Plan for using and disseminating knowledge	24
	Future exploitation plans established	24
	Website and other dissemination materials prepared	24

1.4 Problems encountered during the reporting period, including the corrective actions undertaken

Problems encountered	**Corrective actions taken/proposed**
Field testing was not possible in the intensity and extent due to delays in module prototype manufacturing, so less time was available to perform these field tests.	Focus was on characterising the cells and modules

SECTION 2 Workpackage progress during the reporting period

2.1 Progress on Workpackage #1 - Project Definition

2.1.1 Objectives

Definition of system requirements from an end user point of view, in terms of performance, user-friendliness and possible applications.

- Definition of material specifications: requirements for bifacial c-Si solar cells.
- Definition of cell manufacturing requirements: self-formation theory to the manufacturing of bifacial c-Si solar cells.
- Defining reflector performance requirements.

2.1.2 Progress made during the project

Task worked on	Contractor(s) involved
Definitions on materials used, manufacturing processes (Self-Formation) and reflector design/manufacturing	ALL

Achievements / Progress made on this task

The project has been defined in more exact terms. Starting from end user requirements, the project has been defined with respect to material specifications, manufacturing route and reflector design. More in detail following have been analysed and defined.

MATERIAL:

- Cell dimensions (lab. scale; module scale).
- Efficiency / performance definition.

MANUFACTURING (Self-Formation):

- Interaction matrix is enhanced by new specific modes of interactions in solar cell manufacturing technology.

The basic interaction matrix for solar cell self-formation is included into self-formation simulation software. In this project it will be renewed by interactions of spatial object with finite chaotic medium (soft condensed matter – see Figure 2), and of a homogeneous oriented medium with spatial object (Figure 3).

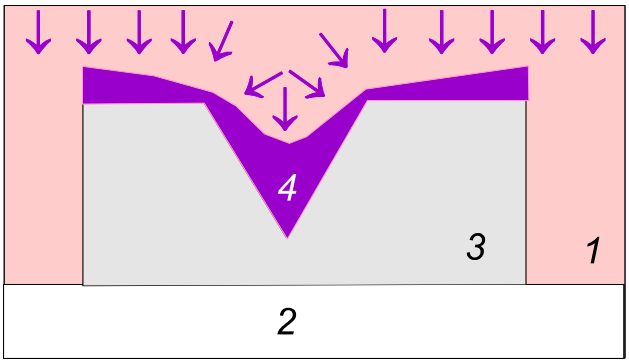

1111	1212	1343^{f}	1444^{f}
2121	2222	2323	2424
3134^{f}	3232	3333	3434
4144^{f}	4242	4343	4444

Figure 2: Finite chaotic medium

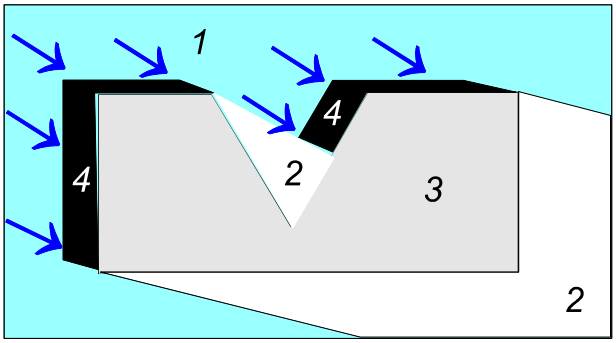

1111	1212	1343$\downarrow^{d}$	1444$\downarrow^{d}$
2121	2222	2323	2424
3134$\downarrow^{d}$	3232	3333	3434
4144$\downarrow^{d}$	4242	4343	4444

Figure 3: Oriented medium

- Its realisation versions have been established in solar cell manufacturing technology.

Finite chaotic medium in solar cell technology can be realised by viscous liquid (photoresist, sol-gel) coating on a spatial wafer by spin-on technique. The oriented medium can be realised as metals oblique evaporation on a spatial object.

- Geometrical and topological features of figures defining selective interaction with one selected medium have been established.

The selectiveness of finite chaotic medium interaction depends on the initial object configuration (depth and width of the grooves), liquid viscosity, its adhesion to the object surface and deposition conditions (spinning velocity, acceleration etc.). From all these features a film irregularity emerges which can be used to another structure established by the self-formation technological process. It has been established that the selectiveness of the oriented medium interaction depends on the particles' flow angle and initial object configuration (groove wall inclination and groove width).

- Algorithms for patterning processes have been defined.

REFLECTOR:

- Dimensions have been defined.
- Physics and basics: choice of fundamental concept is finalised.

A reflector (mirror) will be designed which comes ideally as close as possible to a specular reflector. Physics aspects such as thermal stability, sensitivity to dirt/pollution (sand, bird drops, ...) and corrosion resistance (in particular weather conditions) have been determined, see Paragraph 2.2).

2.2 Progress on Workpackage #2 - Reflector Design and Prototype Manufacturing

2.2.1 Objectives

To design and manufacture a prototype reflector to capture as much albedo sunlight as possible.

2.2.2 Progress made during the project

Tasks worked on	Contractor(s) involved
Analysing functional specifications Defining technical specifications Detailing Reflector design	OP, MILLENNIUM, ISFH, Saules Energija, CRES

Achievements / Progress made on these tasks

The reflector design has been optimised, including:

- Optical design.
- Selection and testing of materials.
- Mounting of cell and module.
- Cooling aspects.
- Exact dimensions; tolerances; surface quality, etc need to be detailed.
- Setting up Manufacturing Plan.

Bifacial solar cells have been used for testing different reflector realisations of the basic design suggested in the proposal. These experiments are supported by optical simulations aiming at the maximisation of the generated current. The basic design is shown in Figure 4.

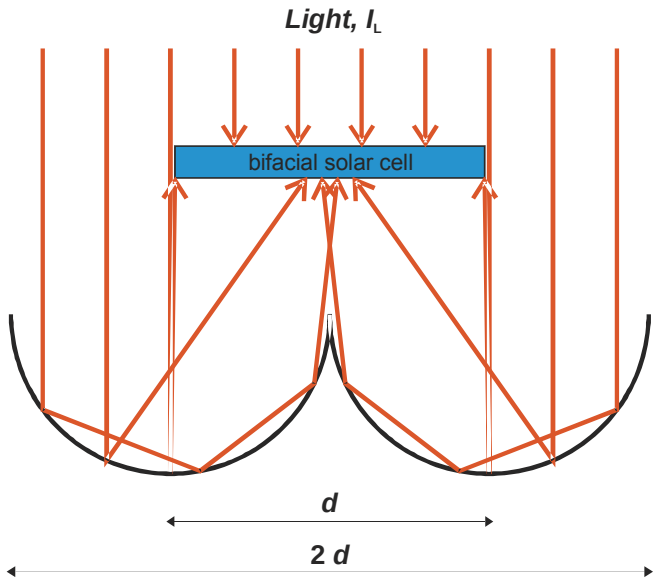

$A_{SC} = d^2$: solar cell surface

$A_L = 2\,d^2$: illuminated area

I_L : light intensity

η_F : front side efficiency

η_R : rear side efficiency

η_t : total efficiency

For ideal reflector and symmetrical solar cell the following is valid:

$\eta_t = 0.5\,(\eta_F + \eta_R) = \eta_F$

Figure 4: Schematic view of basic reflector design

In the following section, the invention and the optimisation of our module design is explained.

The module is made for hosting bifacial solar cells, which means that they are able to receive sunlight from both sides, as indicated in Figure 5. It is well established how the sunlight is incident on the front side. How the light is incident from the rear side, however, depends crucially on the design of the module.

Figure 5: Bifacial solar cells

There has been a long series of module development for bifacial cells.

Bifacial cells can be posted as walls. Figure 6 shows our calculations of the yearly power, depending on the direction the wall is oriented. For example, 90º means that the module's front surface is facing east. Indeed, this alignment is very suitable for bifacial cells, as the sunlight is captured at any time during the day either at the front or at the rear, except during a short period at noon. However, bifacial cells usually convert the light that falls on the rear side less efficiently into electric power than if the light falls onto the front side. This ratio is given in Figure 6 as Eff_{rear}/Eff_{front}. Hence, the curve at the front in Figure 6 with $Eff_{rear} = 0$ represents a monofacial cell, while the curve

at the very rear represents a perfect bifacial cell. Our calculations describe the measurements in Ref. 1 well.

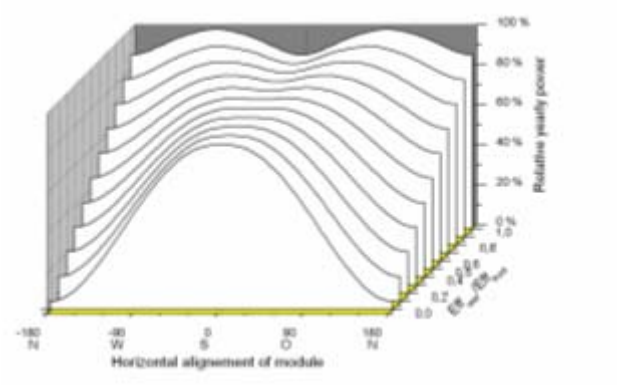

Figure 6: Calculations of yearly power

Another simple design is depicted in Figure 7: sunlight is reflected in a diffuse manner by a white wall at the back. The advantages of this design are simplicity and easy incorporation into architectural design. The disadvantages of this concept are that the cells need to be placed far apart form each other, so they do not shade the wall too much, and that the reflected light has a rather small intensity.

Figure 7: White wall reflector

The rear reflector does not need to be a white wall; it may be a mirror. If this mirror is shaped spherically, all sunrays can be collected by the cell as is shown in Figure 8. This is a clear advantage compared to the designs outlined above. A cell that receives double the light operates under better electrical conditions and, in turn, has a better cell efficiency. Please note, that cell efficiency is defined per cell area. Hence, the bifacial cells in Figure 8 may produce up to double the electric power as a monofacial cell, but their efficiency is not doubled. Experience[2] shows that cell efficiency improves by about 20% relative to the efficiency of a cell that is operated monofacially.

[1] T. Joge et al, IEEE PV Specialists Conference, 2002, p. 1549.

[2] Concept: A. Luque, Solar Cells, 1984, p. 141; recent realisation: U. Ortabasi, 26th IEEE PV Specialists Conference 1997, p. 1177.

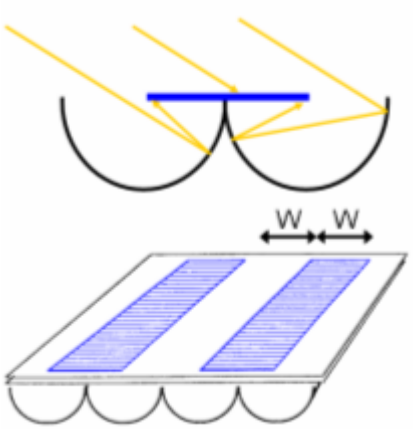

Figure 8: Mirror reflector

While having this advantage, the design has also some disadvantages, which are the reason why it has not been widely used:

- the installation of the cells at the edges of the mirrors poses a challenge.
- Because the mirrors collect the light very efficiently, the cell heats up to about 120ºC (instead of 70ºC as usual) and is only cooled via the surrounding air.
- The entire module is rather bulky to be installed on a rooftop, and collects tree litter etc.
- Last but not least, the sunrays hit the rear side of the cell at rather flat angles in average, where the reflection is rather high[3] (see Figure 9).

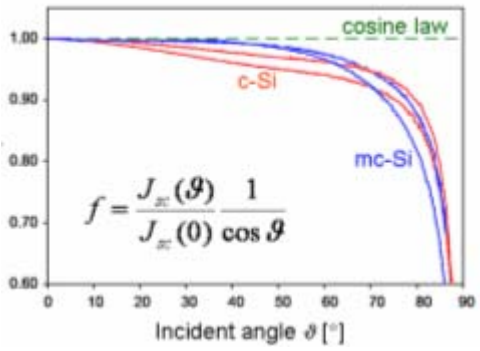

Figure 9: High reflection

Figure 8 calls for designs where the light is concentrated by mirrors. Note that the design in Figure 8 does not concentrate the sunlight: concentration is defined per given cell area, which is double of a monofacial cell. Hence, double the amount of light falls on the double cell area. This is apparent from Figure 8 as well: the width of the cells is equal to the width of the gaps between the cells.

[3] J.L. Balenzategui, F. Chenlo, Solar Ennergy Materials and Solar Cells 86, 53 (2005).

A modification of the above design to achieve concentration is shown in Figure 10. The cell area is clearly smaller than the entrance area of the reflectors. Calculations show that the sunrays hit the cell at steeper angles than in the hemispherical design.

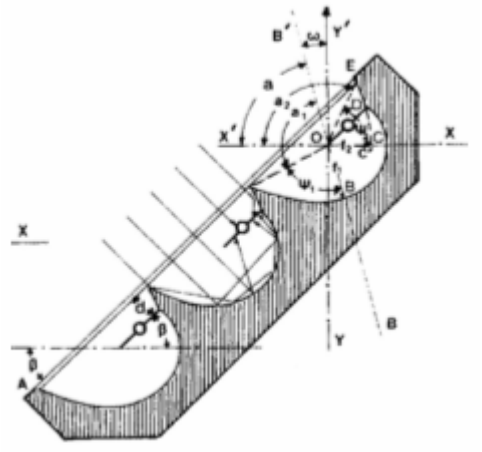

Figure 10: Modification of design

An other design where sunlight is concentrated is sketched in Figure 11: the parabolic trough. Concentration generally improves cell efficiency (if operated at ambient temperature), and the necessary cell area per output power is smaller. However, concentration causes the following two main disadvantages:

- Firstly, the cell is heated up even more than in the above designs. We deal with this further below.
- Secondly, it is impossible to catch sunlight from all directions of the sky. This is due to a fundamental law of optics – the conservation of entendue.

Figure 11: Parabolic design

For the following explanation of the conservation of entendue, refer to Figure 12. The geometrical concentration factor C_g is defined as:

$$C_g = \frac{A_{in}}{A_{out}} \qquad (1)$$

Where A_{in} and A_{out} is are the entry aperture and exit aperture areas, respectively.

The conservation of entendue restricts the relationship between the semi-acceptance angle at entry, Φin, and at exit, Φout, as follows:

$$C_g = \frac{A_{in}}{A_{out}} = n\frac{\sin\phi_{out}}{\sin\phi_{in}} \qquad \text{for 1-dimensional concentration systems} \qquad (2a)$$

and

$$C_g = \frac{A_{in}}{A_{out}} = n^2\frac{\sin^2\phi_{out}}{\sin^2\phi_{in}} \qquad \text{for 2-dimensinal concentration systems} \qquad (2b)$$

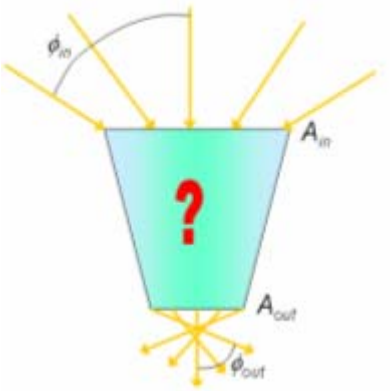

Figure 12: Conservation of entendue

From this follows that the higher the concentration, the narrower is the acceptance angle. This is the reason why highly concentrating systems must track the sun during its daily motion across the sky. Figure 13 shows the upper limit of the achievable entry angle, i.e. for maximum exit angle Φout = 90°.

$$C_g = \frac{A_{in}}{A_{out}} = n\frac{1}{\sin\phi_{in}} \qquad \text{for 1-dimensional concentration systems} \qquad (3a)$$

and

$$C_g = \frac{A_{in}}{A_{out}} = n^2 \frac{1}{\sin^2 \phi_{in}} \qquad \text{for 2-dimensinal concentration systems} \qquad (3b)$$

respectively. For example, we take Φin = 35º in one dimension, such that sunlight can be received during the most of the day without having to track the concentrator. Then the geometrical concentrator factor is 3.5. In this calculation, we use an index of refraction n = 1.5, a representative value for plastic materials. Materials with a higher n are more expensive.

The problem of cell heating has been successfully addressed in the past, as is outlined with some example designs in the following section.

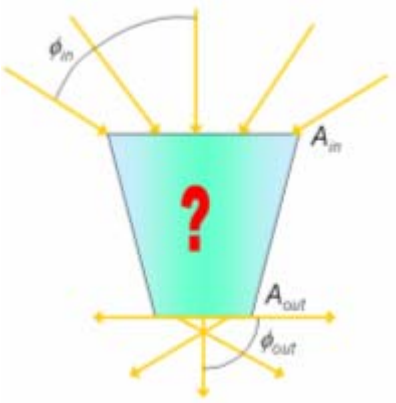

Figure 13: Upper limit achievable entry angle

The trough can be filled with a transparent solid that has a n higher than unity, is depicted in Figure 14[4]. Due to the Law of Refraction, the acceptance angle is larger (dashed line) compared to an empty trough (solid lines) and increases concentration. This explains geometrically why n is involved in equations (2) and (3). Note that n is only involved if the cell is optically linked to the solid having n. If the cell is placed with a gap to the solid, n of the solid is not involved, as the rays are refracted back to the parallel of the incoming rays, following the Law of Refraction.

Filling the trough with a solid has further two advantages:

1. The rays are reflected via total internal reflection, hence no metal coating is necessary to act as a reflector.
2. The dissipated heat of the cell is dispersed to the solid, hence the temperature increase of the cell is diminished.

[4] R.S. Scharlack, Appl. Opt. 16, 2601 (1977).

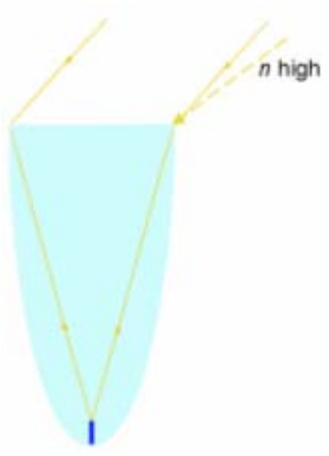

Figure 14: Through filled with solid

The disadvantage is that large amounts of the solid are needed. From geometrical considerations it follows that the produced power is proportional to $C_g WL$, where W is the width and L the length of the concentration system; the depth of the system is proportional to $C_g W$; and the volume to $C_g^2 W^2 L$. Hence, te volume per power is proportional to $C_g W$. Cheap materials have a n = 1.5. For example, if the trough is filled with water, n = 1.3, see Figure 15[5].

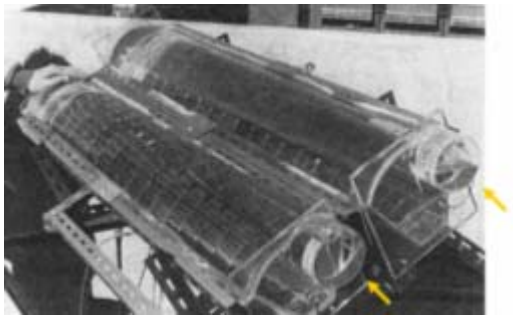

Figure 15: Trough filled with water

Another solid that is used in concentrator systems is glass. An elegant solution is the Venetian blind, as shown in Figure 16-a.[6] It is based on the principle of prisms (Figure 16-b): if the angle δ is sufficiently large, no metallization is needed due to total internal reflections.

[5] I.R. Edmonds, Solar Energy Mat. 21, 173 (1990).

[6] J. Alonso et many al. 29th IEEE PV Conf. 2002, p. 1584.

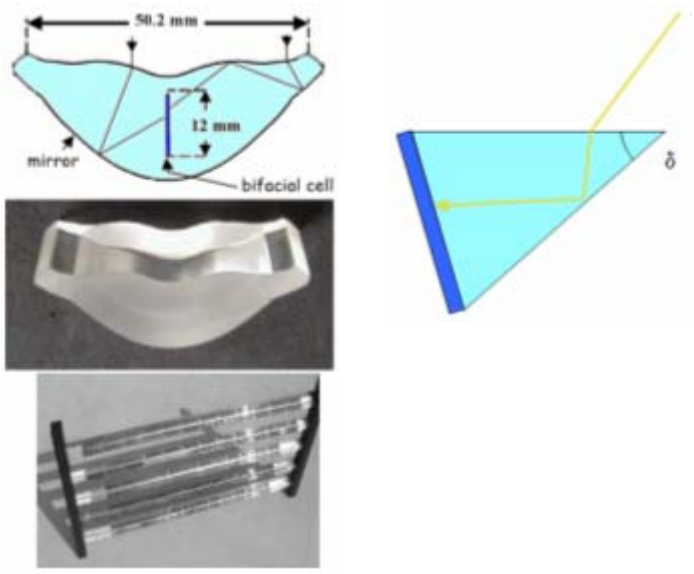

a) b)

Figure 16: Glass used as a solid

A combination of a prism and a trough is shown in Figure 17. In this case, the concentration ratio is the circumference of the prism divided by the diagonal (cell width). The prism is filled with a thermosyphoning dielectric (e.g. water) to cool the cell.

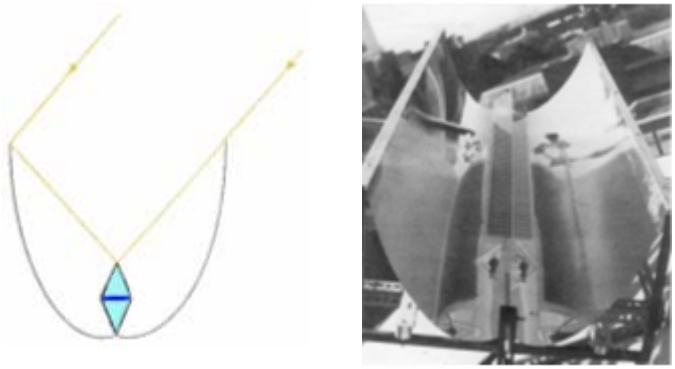

a) b)

Figure 17: Added rear prisms

So far, we dealt with two-dimensional concentrating structures. Three-dimensional structures allow us to achieve higher concentration ratios, as is suggested by Equations (2b) and (3b). An example of a three-dimensional, prism-based structure is shown in Figure 18: rear prisms are added to the main triangular prism, so that a concentration ratio of 2.7 is achieved in a structure that thin to be

usable in roof tiles.[7] The solid is acrylic with n = 1.5, and the rear need to be coated with aluminium as there is not a sufficient amount of total internal reflection in such flat structures.

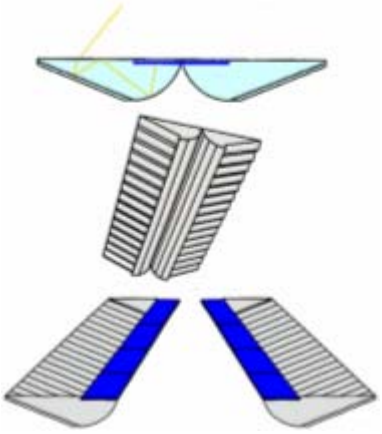

Figure 18: Three-dimensional, prism-based structure

To summarise, a metamorphosis of module designs that point towards our invented design is plotted in Figure 19.

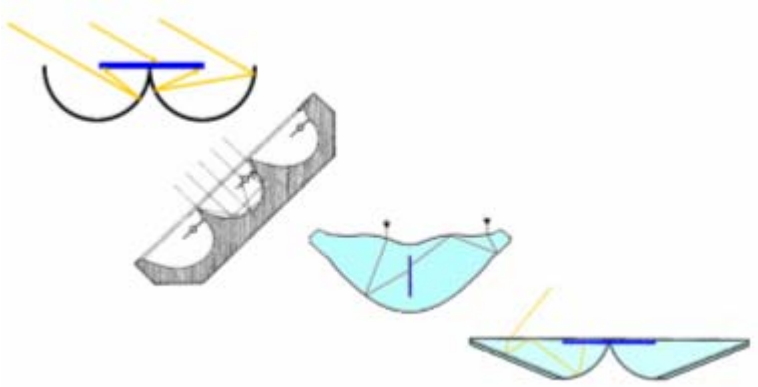

Figure 19: Metamorphosis of module designs

The REFLECTS module design is shown in Figure 20.

[7] S. Bowden et al. 23rd IEEE PV Conf, 1993, p. 1068.

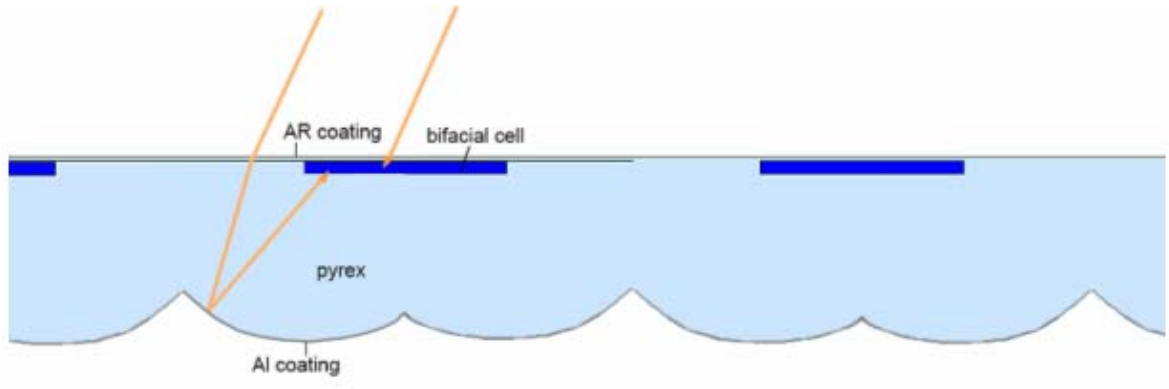

Figure 20: REFLECTS module design

It comprises elements of various designs that have been outlined above: the designs in Figure 8, Figure 10, and Figure 16. The basic idea is that a simple module structure is chosen that can be extruded in one piece per entire module (i.e. the module does not need to be assembled from various pieces). It hosts the cells in a position (at the front surface) that makes it simple to assemble them during module fabrication; note that in the designs of Figure 16 and Figure 17, the cells are buried and accordingly elaborative to assemble. Concentration has been left out, to keep the thickness of the body and, in turn, its weight and costs, to a minimum. Because light trapping is scalable, the wider the cells the thicker the module. Hence, our design prefers relatively narrow, but long collar cells.

The shape of the rear surface required optimization. We used the ray tracer OptiCAD[8], a non-sequential ray-tracer, i.e., the optical components can be assembled freely, so can the light sources. It was sufficient to simulate a geometrically irreducible domain shown in Figure 21.

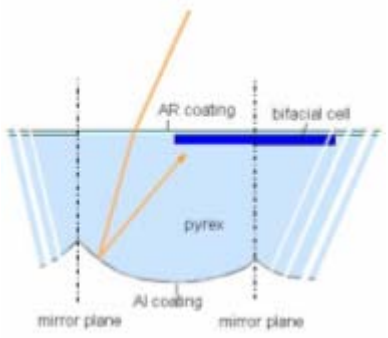

Figure 21: Geometrically irreducible domain

The optical components can be imported from any CAD program and were designed with the EquationEditor. Figure 22 shows an example. The shape of the rear surface was varied and expressed as a sixth order polynome.

[8] OptiCAD Corporation, 511 Juniper Drive, Santa Fe NM, www.opticad.com

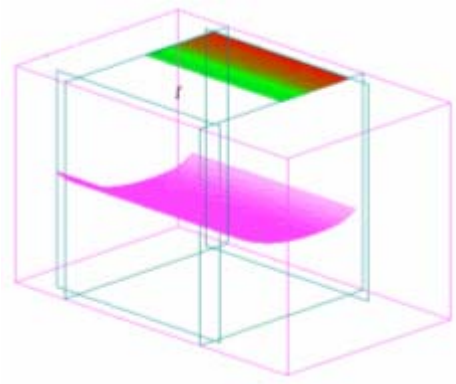

Figure 22: Example design

The geometry of the chosen light source was crucial for the outcome of the optimum module shape. We developed a light-source that represents the sun smeared on the sky over an entire year. We used the atmospheric simulator SMARTS[9] to calculate the standard AM1.5G[10] spectrum. Then we varied the air mass (i.e. the evelation angle of the sun) without changing the components of the atmosphere. This means, we assume that the sky is always blue, and that the atmospheric conditions are always the ones defined by the AM1.5G standard atmosphere.

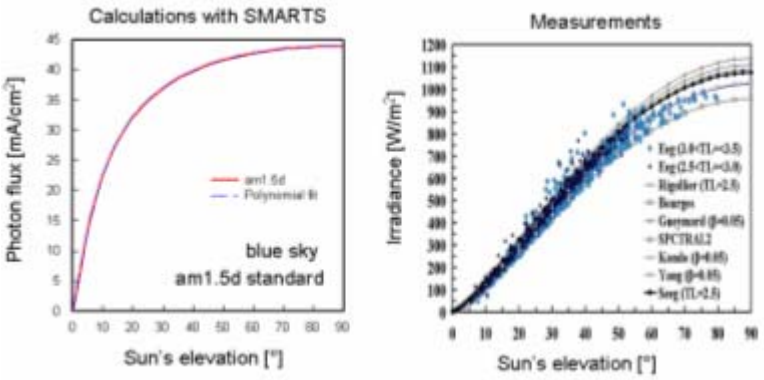

Figure 23: Calculations with SMARTS

Next, we counted the number of photons that are contained in the spectrum between 200 and 1150 nm wavelength. This number (in units of mA/cm^2) is plotted as a function of elevation angle in Figure 23a (left). Figure 23b (right) shows measurements (of the incident power, not the incident photon flux) as given in Ref. 11. The sun was then mathematically smeared on the sky over the entire year. The module was assumed to face south and the celestial equator. The calculated results are shown in Figure 24. The x-axis is the angle on the cell in east-west direction, the y-axis in north-south direction.

[9] SMARTS version 2.9.2, C. A. Gueymard, Solar Consulting Services, Bailey, CO, USA,

http://rredc.nrel.gov/solar/models/SMARTS/relatedrefs/SMARTS292_Users_Manual.pdf

[10] AM1.5G is the standard spectrum of sunlight at the Earth's surface, where “G” stands for "global" and includes both direct and diffuse radiation. The number "1.5" indicates that the length of the path of light through the atmosphere is 1.5 times that of the shorter path when the sun is directly overhead.

[11] N. Igawa a, Y. Koga, T. Matsuzawa, H. Nakamura, Solar Energy 77, 137 (2004).

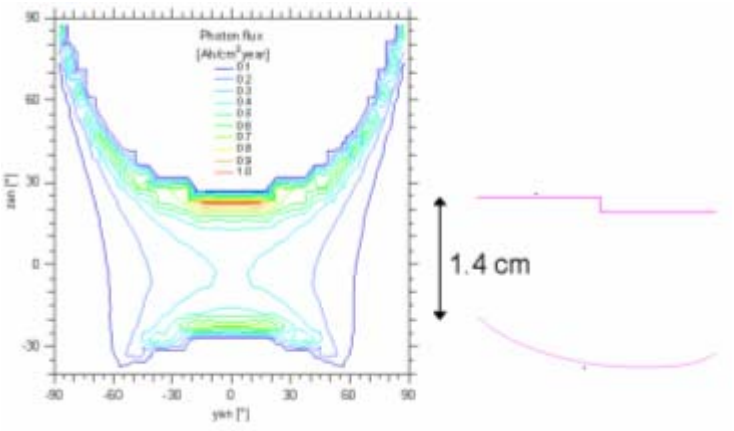

Figure 24: Calculated results

The solid is polycarbonate and the component was manufactured by SME Participant “Optical Products Ltd” (OP). The optical properties of the evaporated aluminium layer at the rear surface were measured at ISFH and are shown in Figure 25 and served as an input for the ray tracing simulations.

The simulations revealed that the best light collection was obtaineded with a rear surface shape described by the following sixth order polynome:

$$y = 1.4+1.012515632x-1.24664905x^2+1.373168391x^3-0.958809832x^4+0.340503952x^5-0.04752691x^6.$$

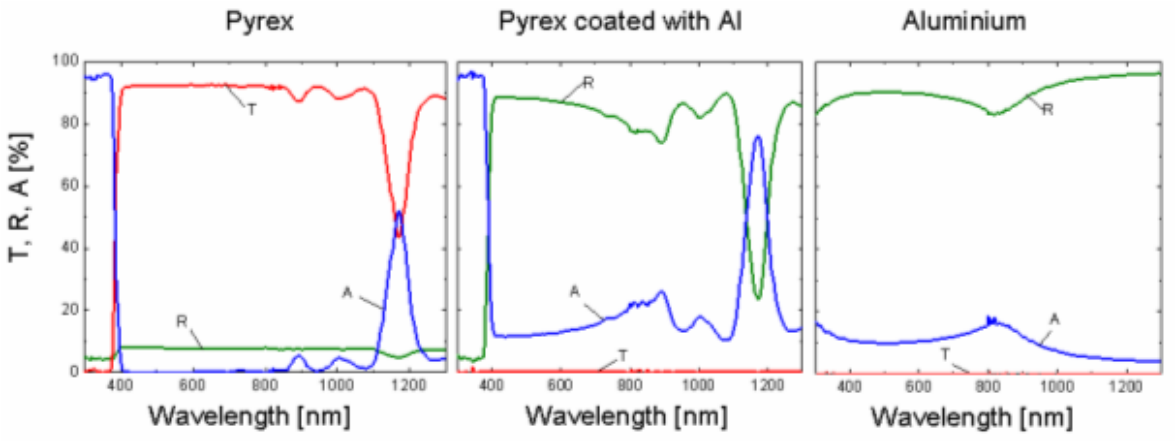

Figure 25: Optical properties

Figure 26 shows the distribution of collected photons at the rear surface of the cell. About half of all photons are incident on the central part, which is a good result considering that the sun is smeared on the entire sky over the entire year. The collection efficiency is close to 80%.

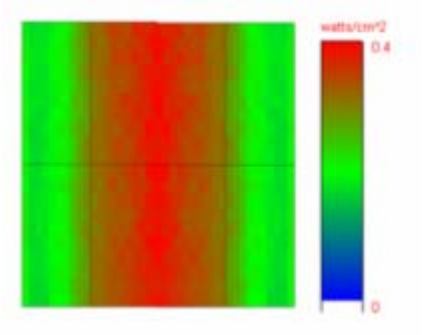

Figure 26: Distribution of collected photons

Task worked on	Contractor(s) involved
Prototype manufacturing	OP

Achievements / Progress made on this task

Prototypes have been made for one promising concepts with respect to their theoretical price/performance ratio, including functional testing.

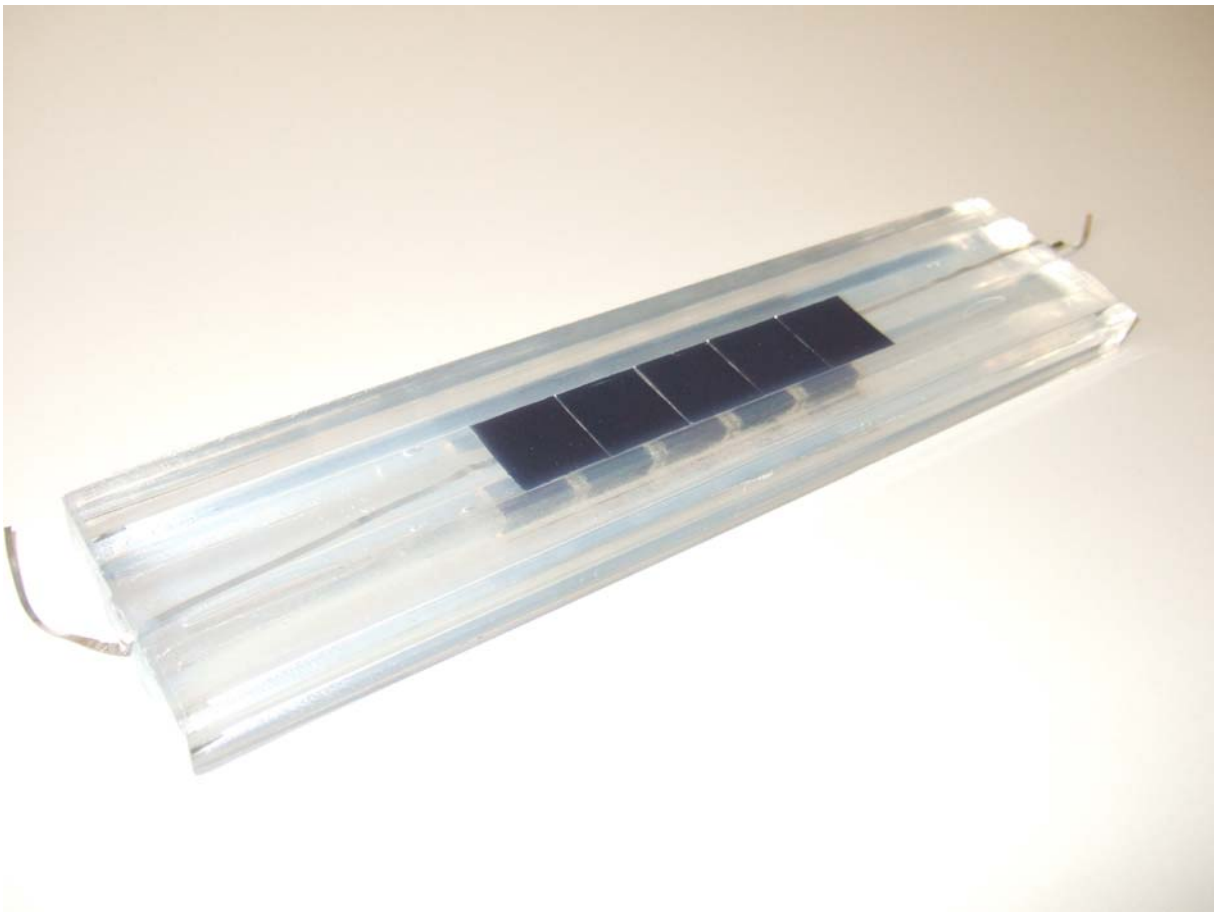

Figure 27: ISFH-ORTO Module with reflector

2.3 Progress on Workpackage #3 - Bifacial Solar Cell ORTO Structure Development

2.3.1 Objectives

- Definition / selection of the best method for mass production of high-efficiency solar cell
  - o Elaboration of spatial solar cell (ORTO-structure)
  - o Elaboration and experimental verification of the requiring self-formation processes
- Definition of the best production process

2.3.2 Progress made during the project

Task worked on	Contractor(s) involved
Defining of the optimal spatial solar cell structure (ORTO-types)	MSI, ISFH, CRES, MILLENNIUM , TELEBALTIKA

Achievements / Progress made on this task

The following subtasks were defined, and progress on these was as follows.

- Define the required initial (starting) object structure.

The ORTO solar cell structure was for the first time defined in the successful HELSOLAR project[12]. In REFLECTS this first structure is referred to as “ORTO-0”). This structure was further researched and some structures, similar to ORTO but with a higher expected efficiency, were introduced. These structured are named ORTO, ORTAN and ORTO-1 (See Figure 28).

The first step of the research to the solar cell structures was a simulation of its fundamental properties (short circuit currents, open circuit voltages, fill factors and corresponding efficiencies). The simulations were performed with ISE TCAD, a software toolbox suitable for this purpose. In this Activity Report only the major findings are reported[13].

The simulation results revealed that the highest structure efficiencies of ORTO-0 are achieved when its base groove has the same dimension as the “fingers’ widths” and the emitter groove width is as wide. If the dimensions are larger, the cell efficiency starts decreasing because the emitter sheet and finger resistances decrease the fill factor; both grooves should be as deep as possible and the elevation width should be as narrow as possible. This dependency is more distinct when the carriers’ bulk life time is higher. This conclusion from the ORTO-0 bifacial solar cell simulations can be extrapolated to the ORTAN bifacial solar cel structure. Since technologically ORTO-0 is a more complicated structure, the simplified ORTO-1 structure was used to compare both structures.

[12] FP5-CRAFT “High-Efficiency Low-Cost Solar Cells”, ENK5-CT-2002-30018.

[13] A detailed report of the simulation results can be obtained from MSI.

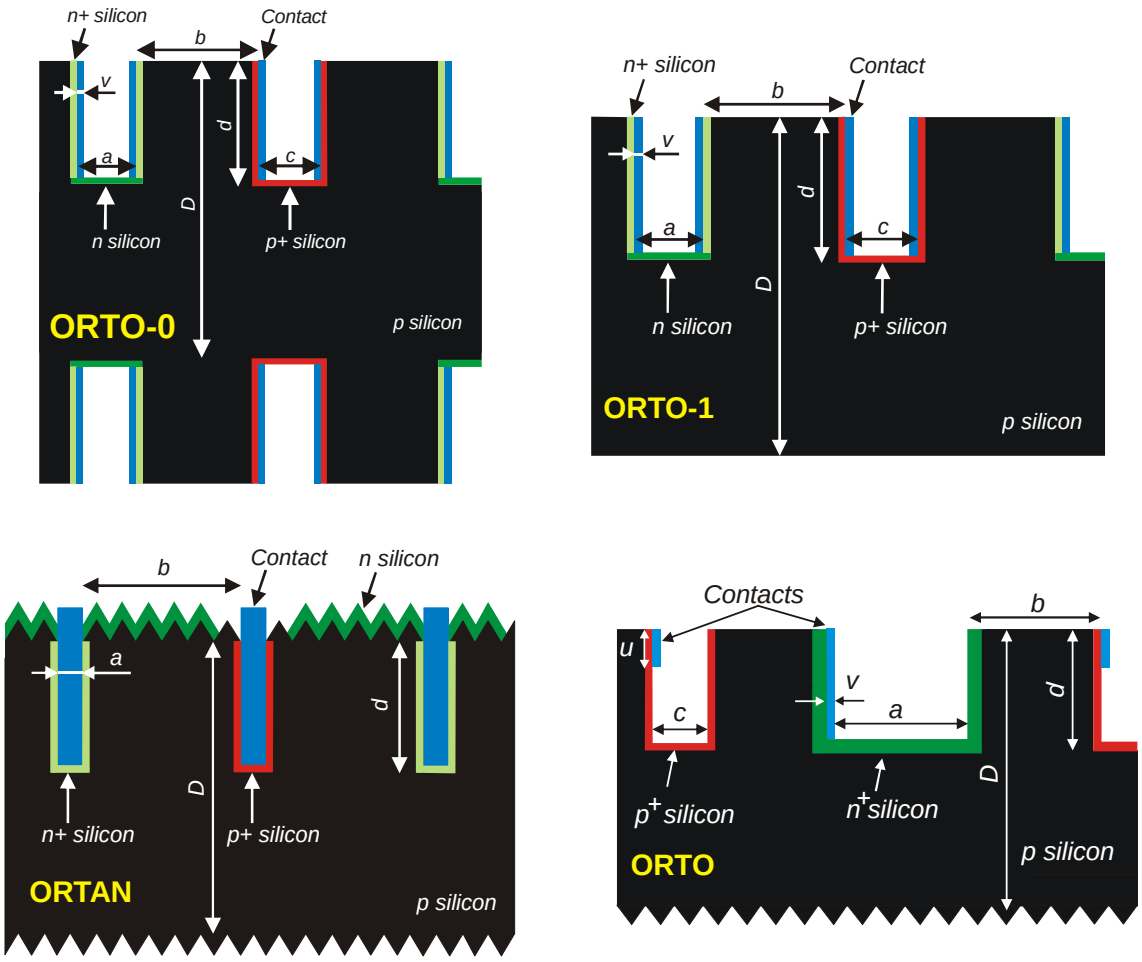

Figure 28: Four bifacial solar cell structures

An ORTO-structure was suggested by ISFH and it was confirmed by simulations carried out by MSI to be the one with highest efficiency potential taking into account a feasible cell production process. In collaboration between MSI and ISFH, a large number of the simulations were performed to find the most optimal geometrical and physical parameters of such solar cell. The cell is as required bifacial but also all contacts are on one cell side. The cell process is kept simple to make it industrial feasible, no masks are needed, no photolithography is necessary.

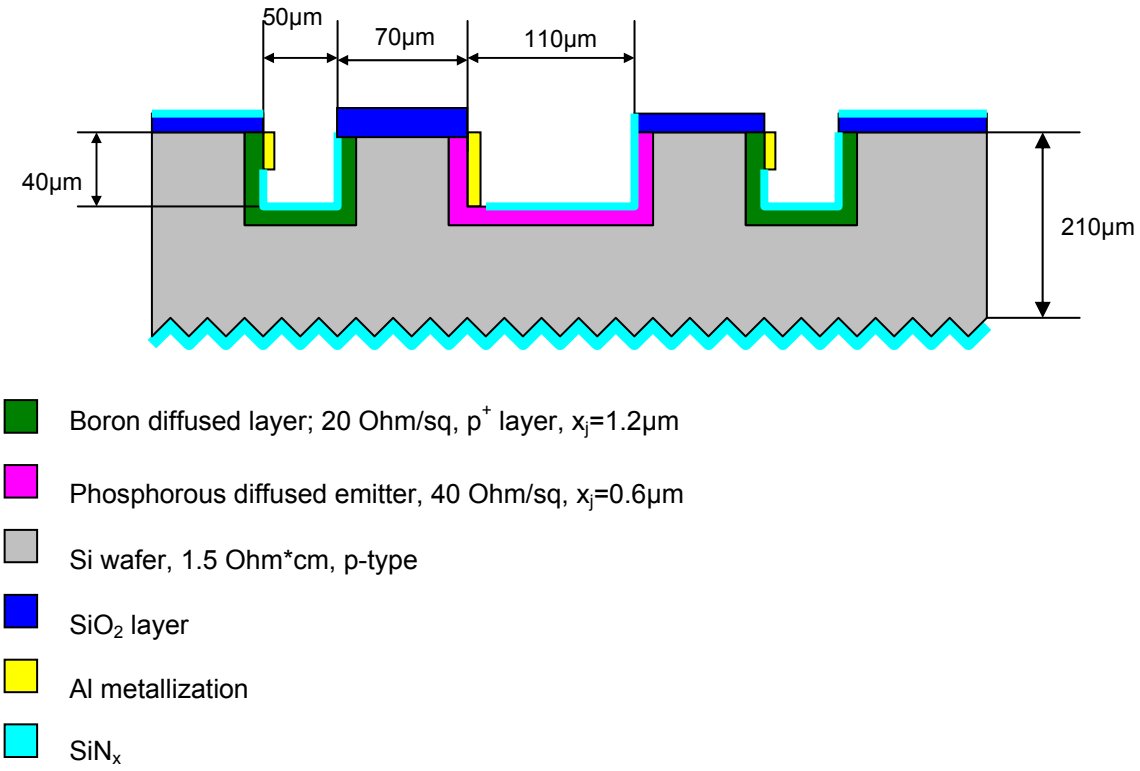

Figure 29: ORTO Cell Structure in detail

The main features of the ORTO cell are:

- *Grooves for cell contacting*: The grooves are formed mechanically by using a conventional dicing saw with rectangular blades.
- *Self aligned metallization:* The contact metal Al is evaporated under a shallow angle. The metal forms metal stripes at the vertical flanks of the grooves.
- *Bifaciality:* Since only contact fingers are formed, that means there is not a full metallization of the on illuminated rear side, the light can enter the cell also from the back.

The major results of the simulations of efficiency for all presented solar cell structures are presented in Figure 31 - Figure 32. Geometrical and physical parameters, which are not shown in the graphs, were optimal for this particular structure.

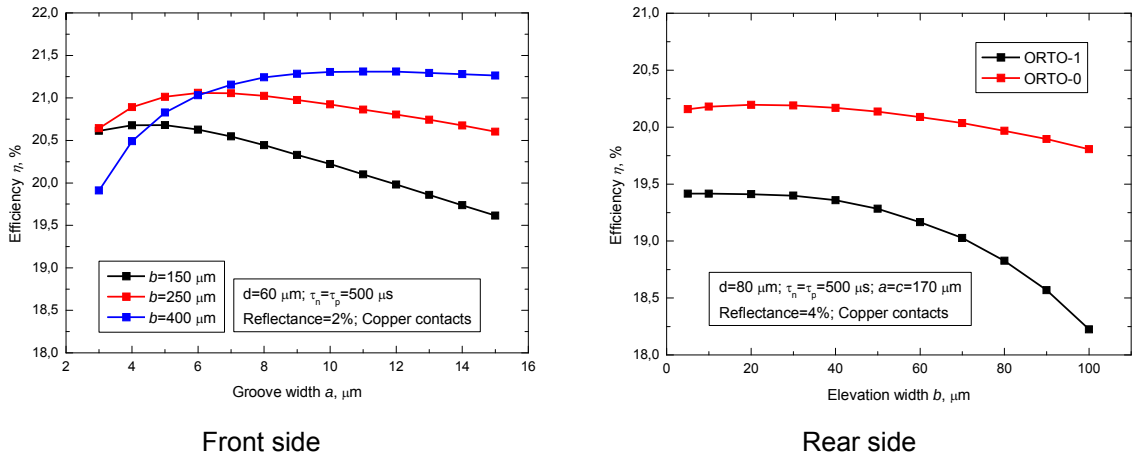

Figure 30: Efficiency dependence on groove width of ORTAN solar cells

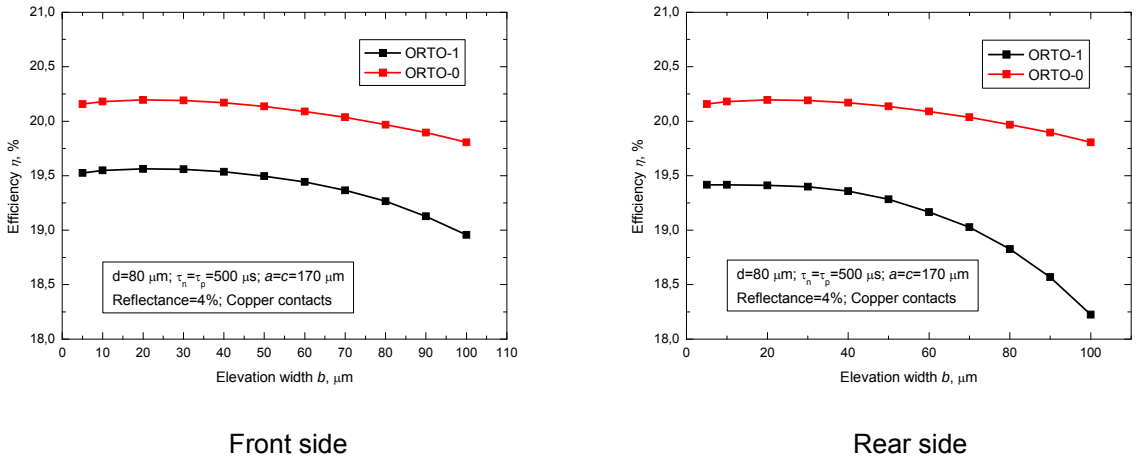

Figure 31: Efficiency dependence on elevation width of ORTO-0 and ORTO-1 solar cells

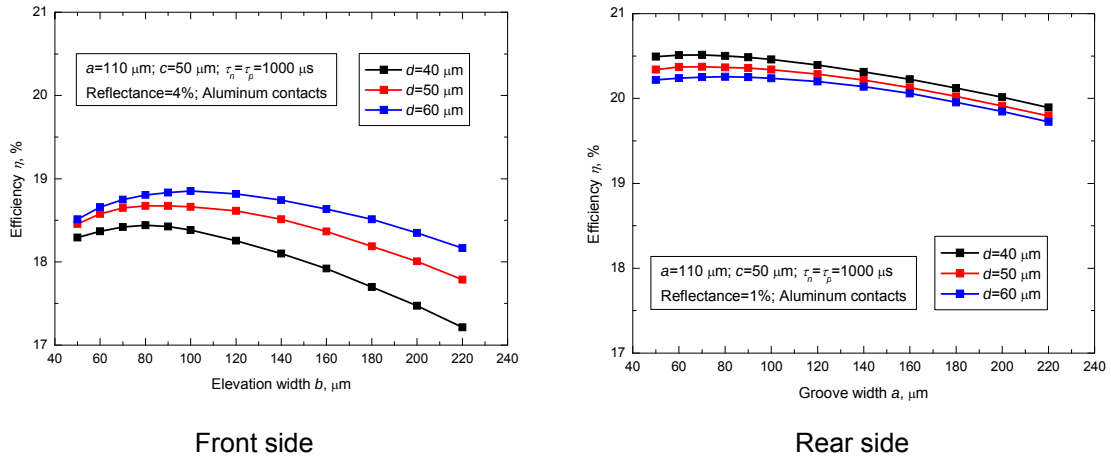

Figure 32: Efficiency dependence on groove width of ORTO solar cells

The comparative efficiencies of all versions are presented in Table 1.

Table 1: Comparison of obtained efficiencies (theoretical)

Version	η_{max}	
	$\tau = 500$ μs	$\tau = 10$ μs
ORTO-0	20.2%	17.4%
ORTO-1	19.5%	17.0%
ORTO	20.5% (1000 μs)	16.3%

The manufacturing processing of the ORTO structures are recommended for patenting.

The main performance and technological characteristics of the examined solar cell versions are presented in

Table 2. ORTO-0 and ORTO-a, b have very similar theoretical efficiencies. ORTO-0 and ORTO-1 require a large number of photolithography steps, which are complex and expensive to perform. ORTO requires only mechanical grooving. Our conclusion is that version ORTO-b is the most favourable.

Table 2: Main performance and technological characteristics of the examined solar cell versions

Version	**η_{max}**	**Patterning**	**Number of patterning processes**	***a, b, c* minimal width μm**	**τ μs**	**Reflec-tance %**	**Si**	**Optimal version under REFLECTS require-ments**
ORTO-0	20.2	Photolitho-graphy	4-6	10	500	4/4	Cz <110>	-
ORTO-1	19.6	Photolitho-graphy	2-3	10	500	4/4	Cz <110>	-
ORTO-a, b	20.5	Mechanical grooving	2	40	1000	4/1	FZ <100>	+

- Determine the required interactions matrix

The interaction matrix **[I]** for ORTO-a and ORTO-b versions differs only by interactions used for creating the solar cell metallization system. In ORTO-a, interaction with an oriented medium is used, and in ORTO-b a finite chaotic medium is applied. The complete structure is introduced in the software program for self-formation simulation. (The entire interaction matrix is too complicated to show here).

The ORTO-a interaction set is written in schemes (1) and ORTO-b in (2) as shown below. Most of interactions are selective. Interacting elements are marked blue (underlined) and non-interacting elements are presented in black. Interaction selectivity is necessary for structure self-formation.

I = {00,00,00,00; 101,05,120,05; 105,05,120,05; 107,05,120,05; 158,05,158,05; 101,19,101,158; 101,21,21,21; 158,21,158,21; 101,027,101,027; 158,027,158,027; 125,027,027,027; 131,027,027,027; 105,027,105,027; 107,027,107.027; 101,50,00,50; 00,36↓^{d},00,36↓^{d}; 101,36↓^{d},101,156↓^{d}; 158,36↓^{d},158,156↓^{d}; 101,55,107,55; 158,55,158,55; 101,56,105,56; 158,56,158,56} (1)

I = {00,00,00,00; 101,05,120,05; 105,05,120,05; 107,05,120,05; 158,05,158,05; 101,019,101,158; 101,021,021,021; 158,021,158,021; 101,027,101,027; 158,027,158,027; 125,027,027,027; 131,027,027,027; 105,027,105,027; 107,027,107.027;105,030,155,030; 107,030,155,030; 120,030,120,030; 158,030,158,030; 155,031,155,150; 101,031,101,150; 158,031,158,031; 101,050,00,050; 101,055,107,055; 158,055,158,055; 101,056,105,056; 158,056,158,056; 101,010^{f},101,140^{f}; 140^{f},070,141,070; 141,016, 016,016; 140,016,140,016, 150,02,151,02} (2)

- Correlate the production parameters to the material properties

Media sequence for ORTO-a is based on oriented media, using:

$I = \{00, 019, 050, 021, 055, 050, 021, 056, 027, 05, 036\downarrow^{d}, 036\downarrow^{d1}, 018\}$

Media sequence for ORTO-b version with self-formed contact windows by finite chaotic medium is based on:

$I = \{00, 019, 050, 021, 055, 50, 021, 056, 05, 010^{f}, 070, 016, 022, 017, 030, 031, 02\}$

- Verify the hypothetical sequences of interaction by iterative simulation runs

In Table 3 materials parameters are presented suitable for ORTO-a and ORTO-b interaction sequences.

Table 3: Materials Parameters for ORTO-a and ORTO-b interaction sequences

Parameter	Material	Parameter	Material
00	Atmosphere	010^{f}	Photoresist solution
019	Gas mixture for PECVD nitride	070	UV light flux
050	Saw blades	016	developer
021	Si etcher	022	SiO_2 etcher
055	Hot boron ambient	017	Photoresist etcher
056	Hot phosphorus ambient	030	Si activation solution
027	P-etcher selectively etching glasses	031	Ni solution
05	Hot oxidizing atmosphere	02	Warm inert gas
$036\downarrow^{d}$	Al atoms flow under d degree		
$036\downarrow^{d1}$	Al atoms flow under d1 degree		
018	Al etcher		

- Define the sequence of interactions for high-efficiency solar cell manufacturing

Hypothetical sequences were verified by iterative simulation runs. The corresponding results are shown in Figure 33 and Figure 34. In the ORTO-a solar cell Al obliquely evaporated contacts are created. In the ORTO-b version the cell contacts are formed by Ni electroless plating.

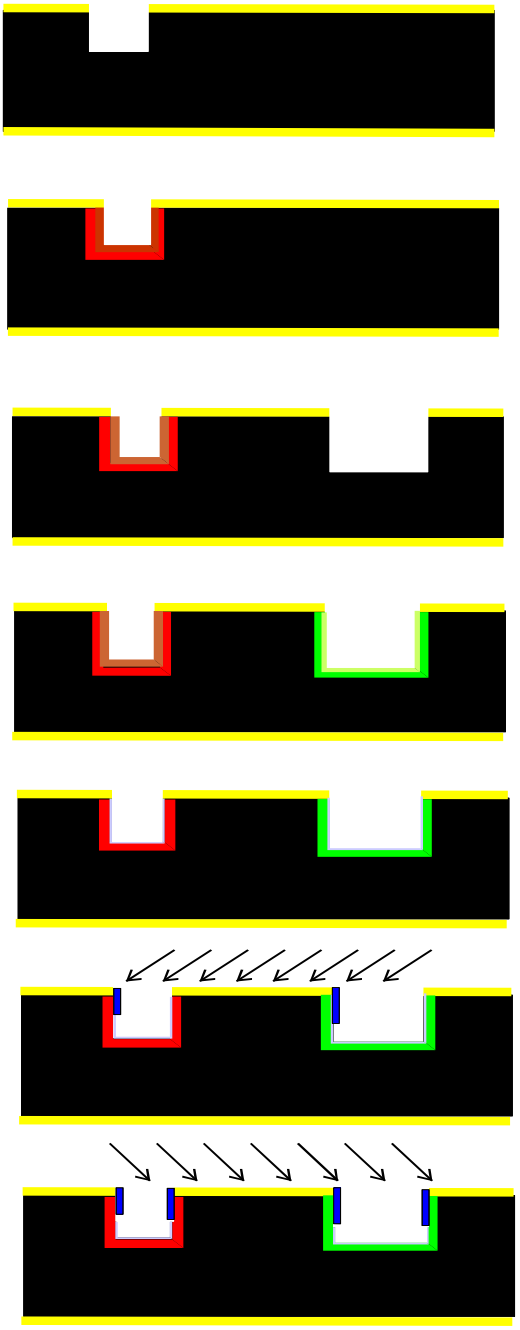

Figure 33: ORTO-a // Version of ORTO solar cell processing with Al evaporation

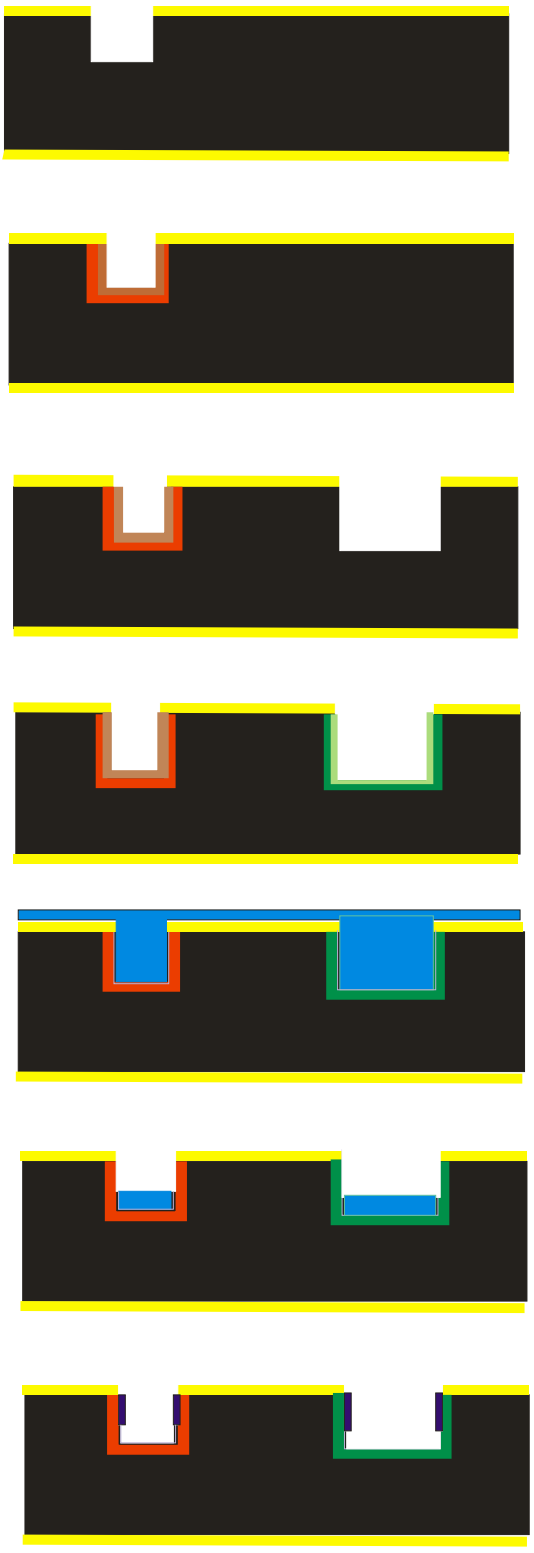

Figure 34: ORTO-b // Version of ORTO solar cell processing with electroless plated contacts

- Select the evolution processes and sequence of homogeneous media

In both versions the first evolution steps are identical. Except grooving, all evolution steps are performed in homogeneous media.

For grid self-formation, oriented homogeneous media $36\downarrow^{d}$ and $36\downarrow^{d1}$ are used in the ORTO-a version. Oriented medium interaction with the grooved object surface creates a non-uniform layer on the object surface. Layer non-uniformity depends on the degree of medium-orientation. Further interaction with a chaotic medium [018] highlights the non-uniformity: the thinnest parts are etched away, while the taller ones remain and form solar cell grid fingers on the grooved walls.

In the ORTO-b version, contact windows for Ni plating are opened by using grooved object evolution in a finite chaotic medium. Finite chaotic medium [010^{f}] forms an irregular cover on the spatial object surface. The contact window height depends on the interaction time of the cover with the next chaotic medium [070] (2), which changes the cover solubility in alkaline solutions. Chaotic medium [016] interacts only with the part of the cover for which the solubility has been changed. Hence, the thicker parts of the cover don't dissolve and prevents the surface part from being etched away in medium [022].

- Correlate the sequence of interactions to available materials and processes

As it can be seen from Table 3: Materials Parameters for ORTO-a and ORTO-b interaction sequences, the oriented media [$36\downarrow^{d}$] and [$36\downarrow^{d1}$] correlates with Al oblique evaporation, where ^{d1} refers to the other evaporation direction. As shown by Hetzel, the Al layer will be thinner as compared to the one groove wall, in case the ion flow direction makes an angle $\leq 45^{0}$ to the plane wafer surface. The other groove wall will be bare. So, if the wafer after Al evaporation will be etched in Al etching fluid while the thinner cover parts is etched, the Al "island" will be formed on the perpendicular wall. However, such result is not only defined by the special ORTO interface, but also by the groove dimensions, allowing metal to be deposited under an angle of less than 45^{0} as well. Only in case of aluminium deposition with an angle less than 45^{0}, the aluminium layer onto the steep flank of the groove will become thicker than a layer deposited onto the horizontal plane. In case of narrow grooves, a deposition angle less than 45^{0} will cause self-formation of the metal structures not on the vertical wall but on the horizontal plane. therefore, for solar cell with narrow grooves such metallization method is not suitable.

The finite homogeneous medium [010^{f}], which creates the possibility to open contact windows on vertical walls, correlates with viscous photosensitive material (photoresist) deposition on a spatial surface by spin-on coating. This method can be used successfully for both narrow and wide grooves, but the open windows area depends on the groove width (assuming the exposition rate is the same).

Below , media sequences for both ORTO versions are displayed as routing cards.

ORTO-a
(with Al metallization)wafer p-type, [100],
1. Wafer texturing
2. Chemical cleaning

3. Silicon nitride deposition on both wafer sides

4. Mechanical grooving

5. Groove cleaning

6. Boron diffusion (not etch away boron glass)

7. Mechanical grooving II

8. Groove cleaning

9. Phosphorus diffusion

10. Boron and phosphorus glasses etching away (selectively)

11. Chemical cleaning

12. Thin oxidation

13. Oblique Al evaporation 1

14. Oblique Al evaporation II

15. Al partial etching

16. Al annealing

ORTO-b

(with Ni metallization), wafer Si [100],

1. Wafer texture

2. Chemical cleaning

3. Silicon nitride deposition on both wafer sides

4. Mechanical grooving I

5. Groove cleaning

6. Boron diffusion (not etch away boron glass)

7. Mechanical grooving II

8. Groove cleaning

9. Phosphorus diffusion

10. Boron and phosphorus glasses etching away (selectively)

11. Chemical cleaning

12. Thin oxidation

13. Photoresist deposition

14. Exposing without photomask

15. Development

16. Oxide etching

17. Ni electroless plating
18. Ni annealing
19. Cu plating

The existing software (developed by MSI in earlier projects) includes technological processes that are approximated by an equidistant evolution model: oxidation of silicon; diffusion of impurities from glasses; diffusion of impurities from gas ambient; isotropic etching; electroless coating; electroplating; etching of monocrystaline silicon with crystallographic orientation <110>; grooving of monocrystaline silicon with crystallographic orientation <100>. The main technological steps developed by self-formation in REFLECTS are: spin-on coating of photoresist, sol-gel glasses on ORTO surfaces, opening contact windows on vertical walls and Ni electroless plating..

- Defining, elaboration and experimental verification of self-formation processes

Elaboration of self-formation processes

Following shows an impression of the work performed during this tasks.

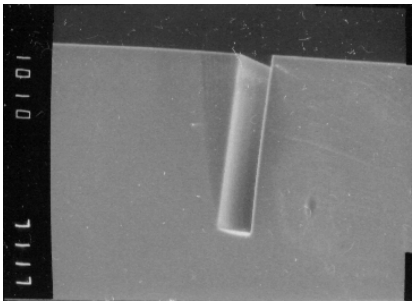

Figure 35: Silicon anisotropic etching

Groove self-formation in silicon bulk by anisotropic etching made according routing card D3.2-1

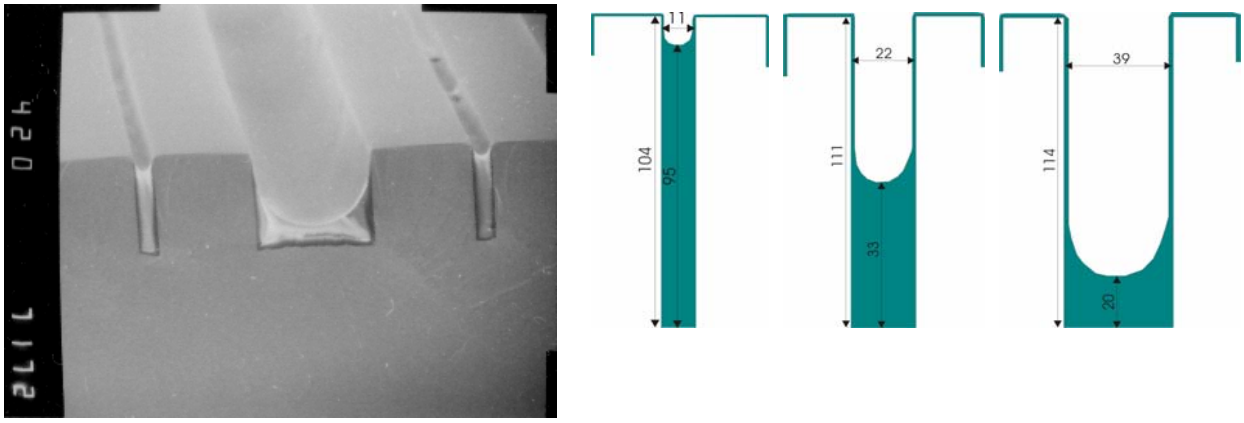

Figure 36: Local photoresist structures self-formation by spin-on coating

Micrograph of photoresist structures under spin frequency 1800 s-1 and corresponding grooves geometry, made according routing card D3.2-3 and D3.2-4

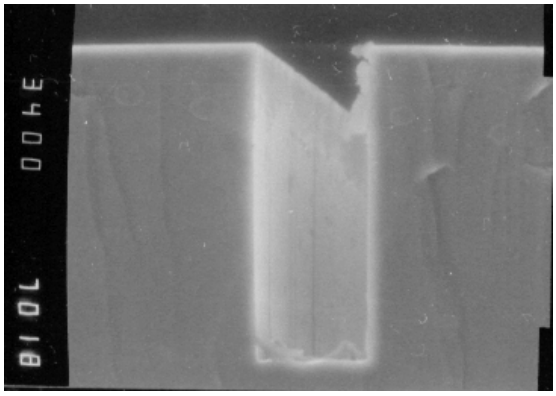

Figure 37: Local doped glasees self-formation by sol-gel spin-on coating

Micrograph of the phosphorous glass layer on the flanks of the ORTO structure groove elevation, made according routing card D3.2-2 and D3.2-6

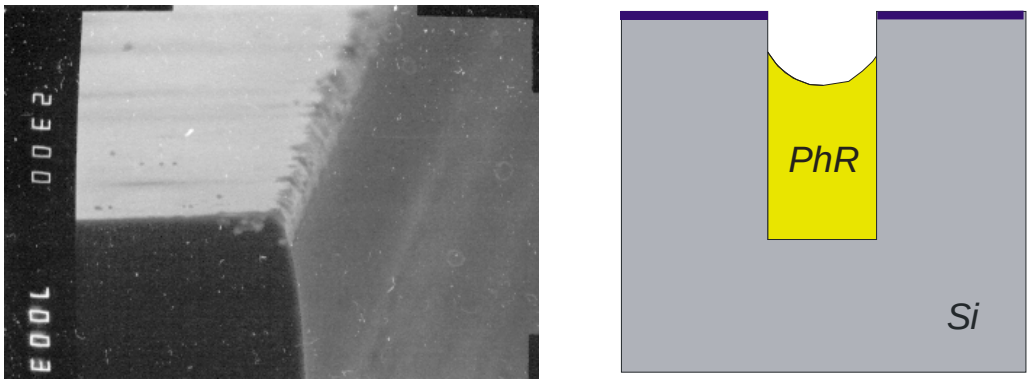

Figure 38: Windows for metallisation self-formation by expose and development of the photoresist structures

Opening of the windows in silicon on the groove vertical wall according routing card D3.2-7

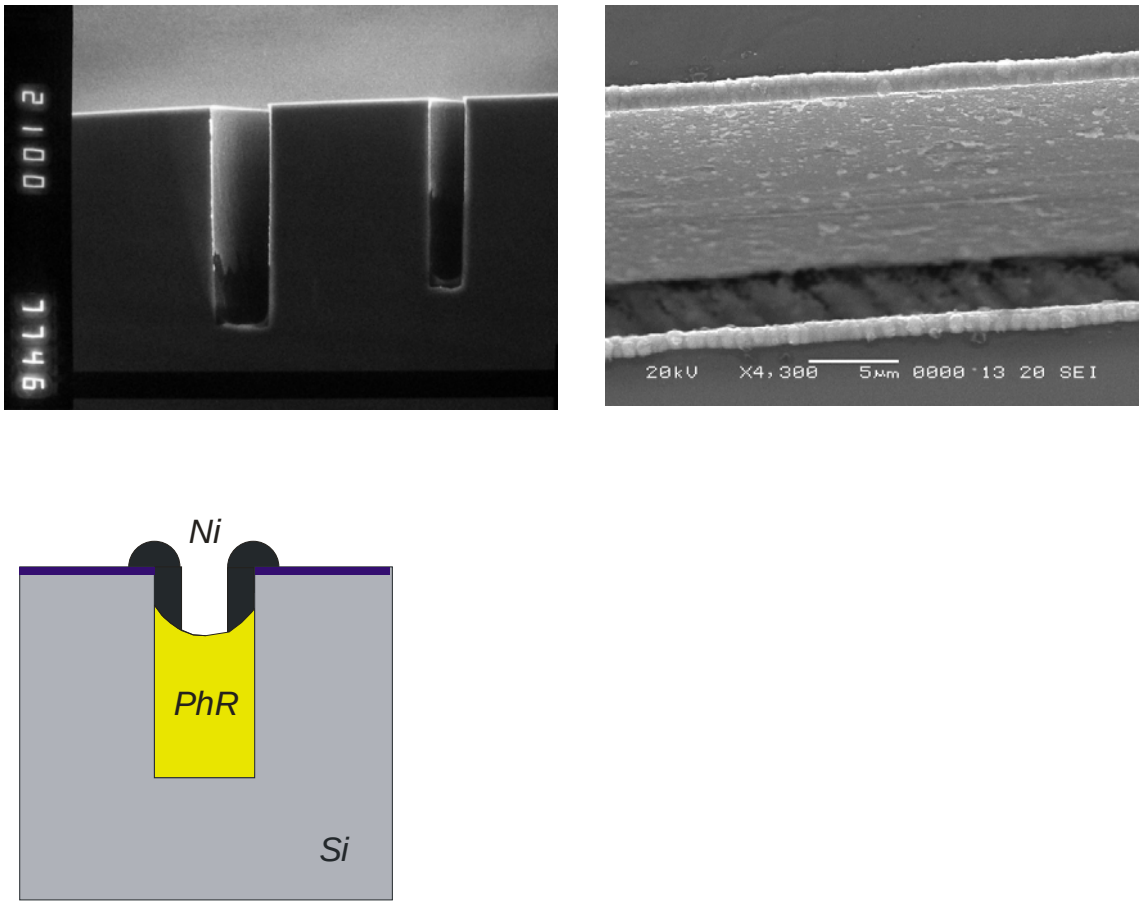

Figure 39: Nickel contacts self-formation by electroless metal plating

The nickel finger deposited by the electroless metal plating technique EMP according routing card D3.2-8

Figure 40: Aluminium contacts self-formation by oblique evaporation (ISFH)

The aluminium finger deposited by the OECO (=oblique evaporation of contact) technique (ISFH)

Table 4: ORTO Routing Cards Overview

ORTO Manufacturing Process	Comments / Remarks
1. Grooves etching in silicon	Annex-1 D3.2-1 Routing card of anisotropic etching Si <110>
2. Spatial surface spin-on coating by boron glass of the permanent thickness	Annex-2 D3.2-2 Routing card of sol-gel boron glass spin-on coating
3. Selective coating of the photoresist, obtaining flat part only under narrow grooves	Annex-3 D3.2-3 Routing card of the photoresist overflow by spin-on coating
4. Selective exposition of the photoresist	Annex-4 D3.2-4 Routing card of the photoresist selective exposition
5. Development of photoresist	Annex-5 D3.2-5 Routing card of the photoresist development
6. Spatial surface spin coating by phosphorous glass of the permanent thickness	Annex-6 D3.2-6 Routing card of sol-gel phosphorous glass spin-on coating
7. Opening of the windows to silicon on the groove vertical wall	Annex-7 D3.2-7 Routing card of the windows self-formation
8. Nickel electroless coating	Annex-8 D3.2-8 Routing card of the nickel electroless plating

Task worked on Contractor(s) involved

Determine the requirements of photomasks

Achievements / Progress made on this task

In case of mechanical grooving the shape and dimensions of the saw blades (not photomasks) determine the patterns in the silicon wafer.

Photoresist spin-on coating on the ORTO interfaces Photoresist FP-9120-2 was used in the experiment. The viscosity of photoresist is 29-34 mm/s (25^0C).

After the photoresist had been released one minute delay before span silicon specimen was taken into account to allow the photoresist to fill the grooves.

Experimental results (all measurements are shown in micrometers)

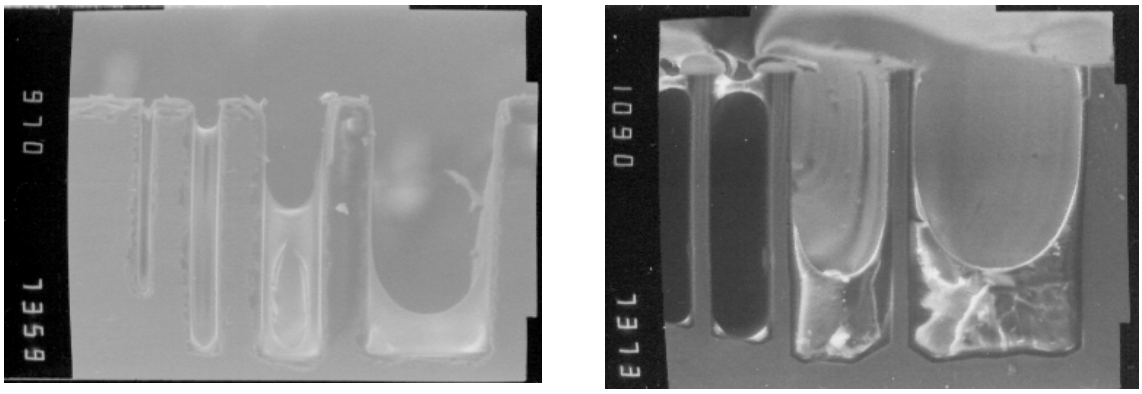

Figure 41: Micrographes of photoresist structures under spin frequency 1000 min^{-1} and corresponding images

Photoresist depth *d* as a function of groove width *a* (spin frequency 1000 s^{-1} can be approximated by following formula:

$$d(a) = 27{,}73 + 177{,}31 \cdot \exp\left(-\frac{a}{12{,}12}\right)$$

[Eq.] 1

Comparison of experiment data with approximated function is shown in Figure 42.

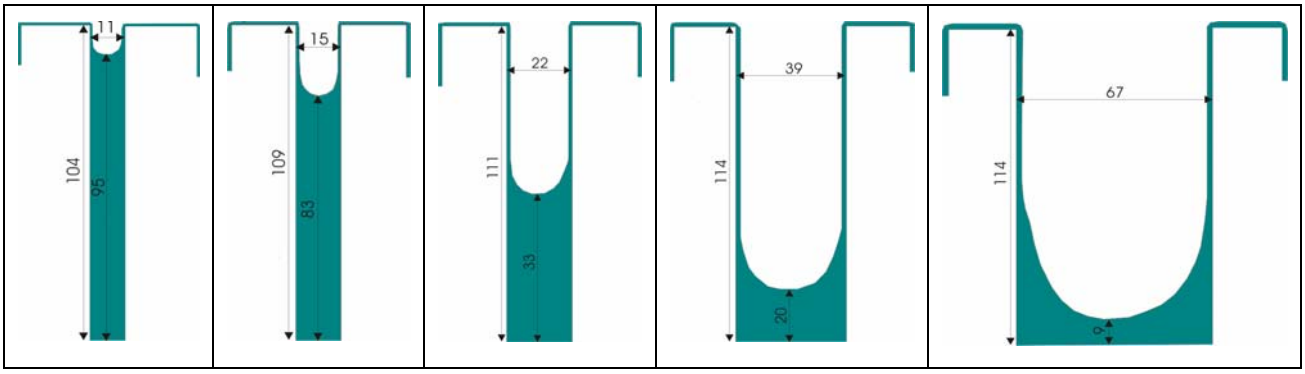

Figure 42: Micrographes of photoresist structures under spin frequency 1800 min^{-1} and corresponding images

The photoresist depth *d* as a function of groove width *a* (spin frequency 1800 min^{-1}) can be approximated by the following formula:

$$d(a) = 9{,}19 + 244{,}62 \cdot \exp\left(-\frac{a}{11{,}03}\right)$$

[Eq.] 2

Comparison of experiment data with approximated function.

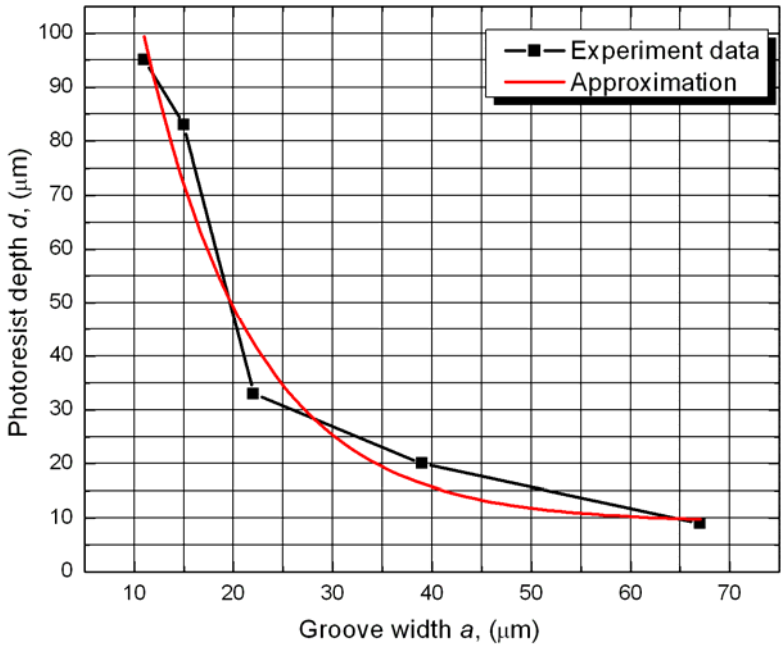

Figure 43: Experimental data and its approximation undera spin frequency of 1800 min^{-1}

Non-permanent spatial photoresist expose simulation. The main function is to simulate exposition of a non-permanent spatial photoresist in ORTO structure. This module is derived from the Routing Card simulation module.

2.4 Progress on Workpackage #4 - Software Development for Self-formation Iterations

2.4.1 Objectives

- Development/setting up of main documents related to software development process
- Architecture design
- Preparation of documents for entire system integration and qualification testing, based on functional requirements (input for this workpackage)
- Development of computer program for simulation of the solar cell self-formation manufacturing methods by iterative process
- Development of computer program for synthesis of optimal initial planar system and technological processes

2.4.2 Progress made during the project

Task worked on	Contractor(s) involved
Development/setting up of software development process related documents	MSI

Achievements / Progress made on this task

Software Development Process related documents are defined as follows:

- Software development plan
- Software quality attribute tradeoffs analysis
- System requirements specifications
- System architecture
- System overview
- Software design document
- Integration plan
- Templates for system testing protocols

- List of current top risks
- Quality Assurance Plan
- Coding Standard

Task worked on	Contractor(s) involved
Analysis of acceptable tradeoffs between competing attributes	ISFH, MSI

Achievements / Progress made on this task

The extent to which particular software reaches its quality goals can be characterized by certain attributes.

The following attributes were considered when evaluating implementation strategy for self-formation simulation:

1. Correctness / Accuracy - how accurately the selected models relate to real processes being simulated
2. Robustness / Reliability - the level of software ability to correct operational mistakes, erroneous input data, and hardware errors.
3. Usability / User friendliness - how easy a user can operate with the software
4. Efficiency / Performance - how efficiently software utilizes all necessary resources (cpu time, storage, etc), how fast are the simulations
5. Maintainability / Testability - How easy, without undesirable side effects, software can be maintained (error fixes), or modified
6. Portability - how easy software can be adapted to other platforms
7. Extensibility - how easy new functionality can be added to the software

Focusing on some attributes affect other attributes positively or negatively. The summary is provided in Table 5.

Table 5: Comparison of self-formation simulation software attributes

	Correctness/ Accuracy	Robustness/ reliability	Usability/ User friendliness	Efficiency/ performance	Maintainability / Testability	Portability	Extensibility
Correctness/ Accuracy	**X**			**down**			
Robustness/ Reliability	**X**	**X**		**down**	**down**		**down**
Usability/ User friendliness	**X**	**X**	**X**	**down**	**down**	**down**	
Efficiency/ performance	**X**	**X**	**X**	**X**	**down**	**down**	**down**
Maintainability/ Testability	**X**	**X**	**X**	**X**	**X**	**up**	**up**
Portability	**X**	**X**	**X**	**X**	**X**	**X**	**up**
Extensibility	**X**	**X**	**X**	**X**	**X**	**X**	**X**

According to the functional specifications the priority of attributes is as follows (higher to lower):

1. efficiency, accuracy
2. extensibility, portability
3. maintainability, user friendliness, reliability

It is obvious that balancing between efficiency and correctness / accuracy is the most difficult, since these attributes mutually contradict.

The strategic approach taken in this implementation of self-formation simulation is as follows:

- define and adhere to the absolute minimum of performance requirements
- then define minimum of accuracy requirements

Task worked on	Contractor(s) involved
System architecture design	MSI

Achievements / Progress made on this task

Subtasks

– Definition of components and properties for each component in the system. System views.
– Data flow diagram.
– Collaboration diagram.
– Specification of internal and external interfaces for the system.
– Evaluation of development/runtime tools/platforms, requirements for PC hardware.

Components

The Self-formation simulation system consists of the following components:

- simulation control
- simulation data
- data forms
- evolution mechanism
- repository of interactions
- repository of parameters
- visualization

The control module initiates two different scenarios – data editing or simulation. Data editing operates on project related data or global data. This component provides editing of configuration of simulation object, light masks, interaction set, parameters and media sequence.

Simulation operates on grid data by invoking functions from evolution mechanism component. Certain user related functions, such as evolution by step, etc are also provided.

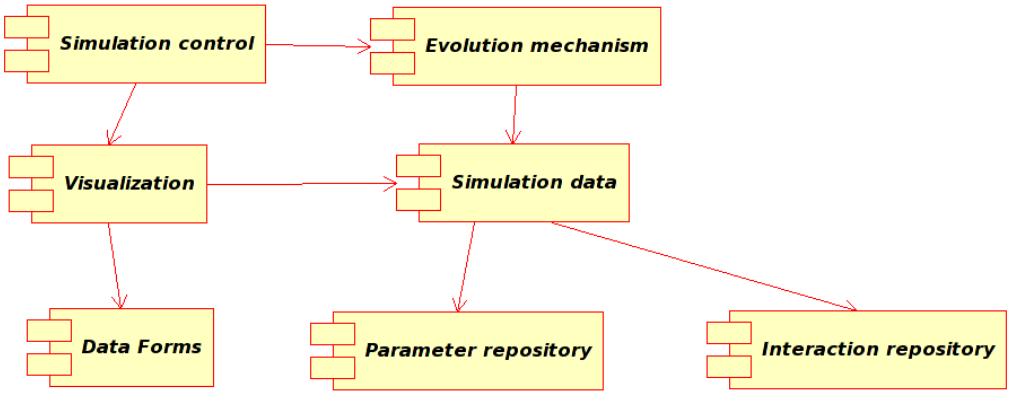

Figure 44: System blocks

Use cases

The use cases that can be used within the system are as follows:

- Enter global data
  Set up *Parameter repository* and *Interaction repository*
- Enter project related data
  Set up initial media sequence, set up object contours and light masks
- Perform self-formation simulation
  Step-by-step simulation or continuous simulation

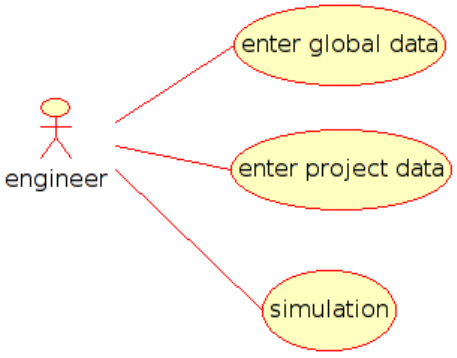

Figure 45: Use cases

Simulation scenario

Self formation simulation is the main function performed by the software. Sequence and collaboration diagrams are visualised in Figure 46 and Figure 47 respectively.

Schematically the first action goes out from Simulation Control component – to initiate the operation. Simulation data grid is reset. Then the Simulate command is issued which runs in a

loop. The loop is determined by Media Sequence of project related data. The simulation must run for each medium from the medium sequence for the specified time interval. In parallel contents of simulation data are displayed for monitoring purposes. The operator always has possibility to cancel the simulation loop.

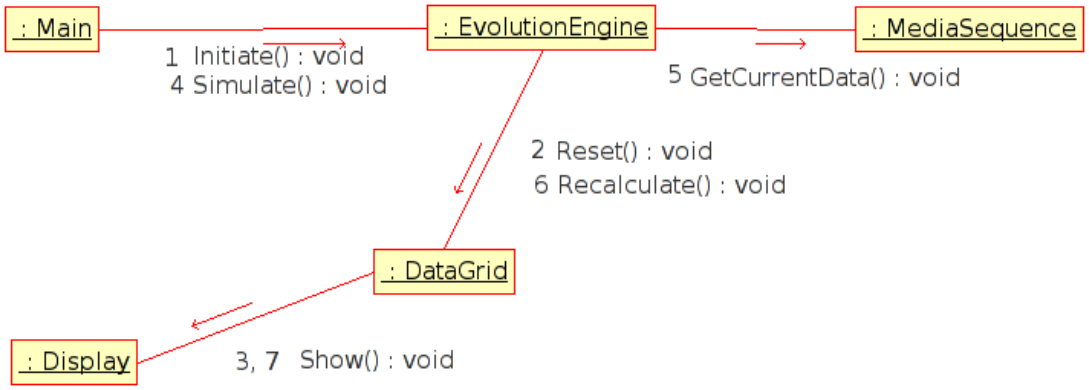

Figure 46: Sequence Diagram

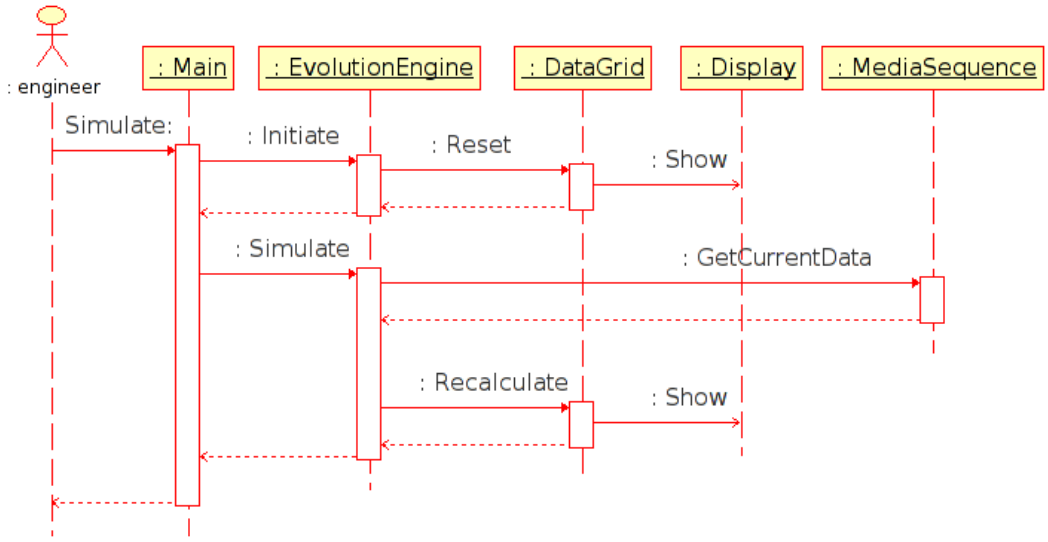

Figure 47: Collaboration Diagram

Memory usage considerations

This design suits the current requirements based on a typical object of simulation – a solar cell cross section of dimensions approx 300 micrometers by 1000 micrometers. The object is represented by a grid. The precision is determined by number of cells for each square micrometer. Since some technological processes being simulated create layers of thickness of order 0.1 micrometer, a cell of reasonably precise grid should correspond to 0.01 – 0.1 square micrometer.

Therefore this amounts to 600 MB for one plane - height 300 by width 1000 by 100 (cells for one micrometer) by 20 (approx data structure size). This is significant amount, both in terms of memory space and processing time.

Since the majority of cells are not used in an evolution cycle, a special technique – blank super cells are introduced. The super-cells are squares of cells, with configurable height. It is assumed that each cell in a super cell consists of the same colour and is not in an excited state. Therefore a super-cell (i.e. a collection of cells) is represented by one single structure. When interaction occurs in a neighbourhood of super cell, the super cell is converted to simple cells. Likewise, a group of cells routinely may be converted to a super-cell. Such technique dramatically reduces memory and calculations.

Task worked on	Contractor(s) involved
Development of system requirements specification	TELEBALTIKA, MILLENNIUM, MSI

Achievements / Progress made on this task

– Functional requirements for entire system.

– Special requirements for the system (system throughput, real time, data integrity, ...).

Software in REFLECTS is viewed as an aid in the technological design of a bifacial solar cell, created on the basis of the ORTO structure. The software is not supposed to replace real experiments - rather decrease their number and provide guidance to fundamental decisions in technology design.

The main software functions are as follows:

- Silicon oxidation
- Photoresist overflow
- Photoresist spin-on coating on flat and ORTO surface
- Photoresist exposition in light stream with photomask
- Photoresist exposition in light stream without photomask
- Development of exposed photoresist
- Etching, removal of photoresist
- Si <110> anisotropic etching
- Si <100> mechanical grooving
- Si isotropic etching
- ORTO surface coating by Sol-gel glasses
- Glass etching
- p,n diffusion from glasses in silicon

- p,n diffusion from gas medium in silicon
- Chemical coating of metal
- Electroplating of metal
- Metal coating by epitaxy

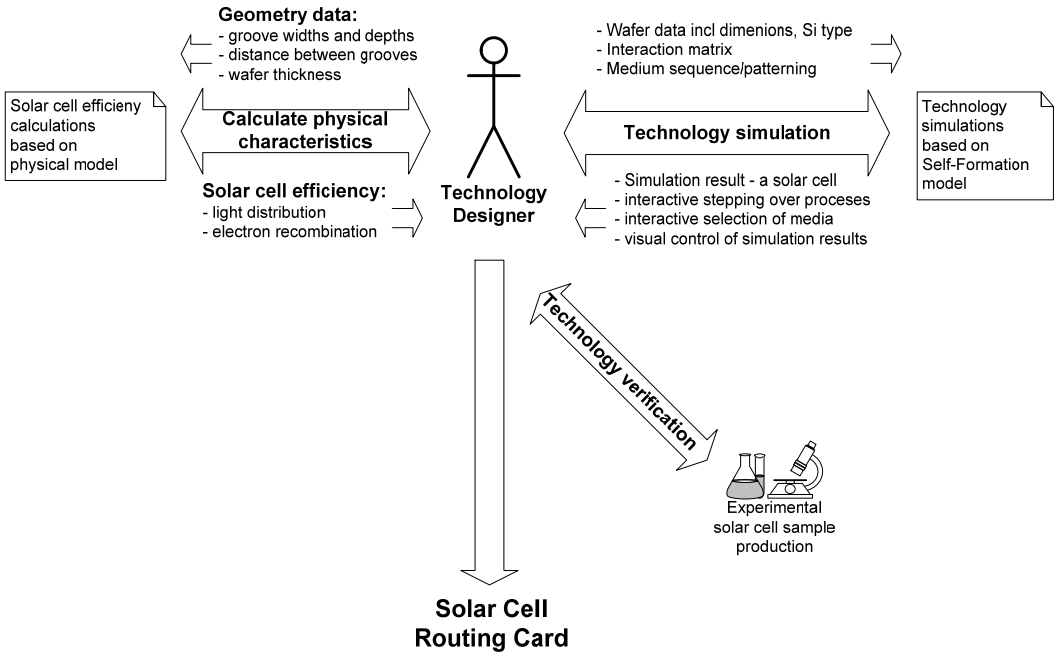

Figure 48: Technology development scenario

All simulations are performed in a 2D cross-section. The principle structure of the solar cell top (bottom) is provided below.

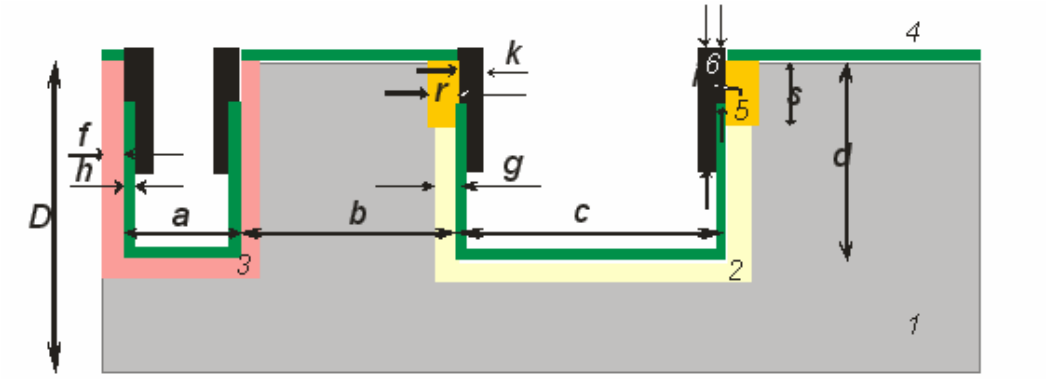

Figure 49: Orthogonal (ORTO) structure.

***1* –monocrystalline silicon *p* – type; *2* – emitter *n* - type; *3* – basis p^+ - type; *4* – antireflection and passivation oxide; *5* – emitter n^+; *6* – emitter and base contacts**

The purpose of the Routing Card simulation is to find the optimal sequence of media leading to the desired target structure of the bifacial solar cell.

The following forms are used for the main use cases and data management:

- Technological process management:
  - load/save selected technology (parameters, interactions)
  - edit parameter set
  - edit interactions
- Project data and media sequence editing
  - load/save selected project (media sequence, initial object, photomask templates)
  - edit/create media sequence
  - save data
- Simulation control and monitoring:
  - step by step simulation of evolution
  - automatic simulation of evolution
  - step back to previous evolution state
  - visualization of object change in the course of evolution
  - zoom in/zoom out
  - identification of materials of the displayed object (by colors and/or ToolTips)

Simulation data consists of two data groups:

- technology related data
  - parameters
  - interactions
- project related data
  - initial object / figure
  - media sequence
  - transformation templates (information related to evolution simulation)

Project data is maintained for each model. Technology data is supposed to be uniform for all projects, but can also be changed, if new technology is introduced. In the latter case the user has to ensure compatibility.

The main result of simulation is media sequence. The media sequence must be available for viewing on screen, along with specific state of the object, i.e. what the object will be if evolution ends with that medium. The media sequence must be available for export in text or pdf file format. The deliverable is a standalone application, providing input of required parameters, routing card simulation and display of results.

Task worked on	Contractor(s) involved
Preparation of software system integration plan	TELEBALTIKA, MILLENNIUM, MSI

Achievements / Progress made on this task

The software system integration plan, integration test plan and integration testing protocol template, entire system qualification test plan and testing protocol template needs to be developed. The system integration plan provides a view of the various steps that are necessary to obtain a correctly functioning system. The following elements are addressed in the plan:

- site preparation
- hardware preparation
- training and education
- prototype production
- verification of functionality
- optimization of the system performance
- pilot testing
- full installation

System Integration testing plan defines testing environment, tools, tasks, error management. Testing of the system consists of the following parts:

- testing of data entry forms
- testing of standard circular evolution
- testing of diffusion evolution
- testing of soft matter evolution
- testing of heating process
- testing of sample solar cell routing card

When any part of the system is changed all tests have to be repeated.

The System Integration Testing Protocol must include the following:

- Date of the testing
- Person who conducted the tests
- Tests conducted
- Number and list of priority 1 bugs
- Number and list of priority 2 bugs
- Number and list of priority 3 bugs

Task worked on	Contractor(s) involved
Develop software program for simulation of structure/pattern evolution in plane and between planes.	MSI, ISFH

Achievements / Progress made on this task

This program provides a tool for fast analysis / verification whether a particular chosen approach would lead to the desired result. The analysis is based on calculating the theoretical light absorption by a spatial surface and the associated electrical performance of the solar cells. Moreover, it enables optimisation of the patterning process through iteration.

Self formation simulation software was created. The software simulates self-formation based technological processes for manufacturing of spatial solar cells and can be used in elaboration of new spatial solar cell structures.

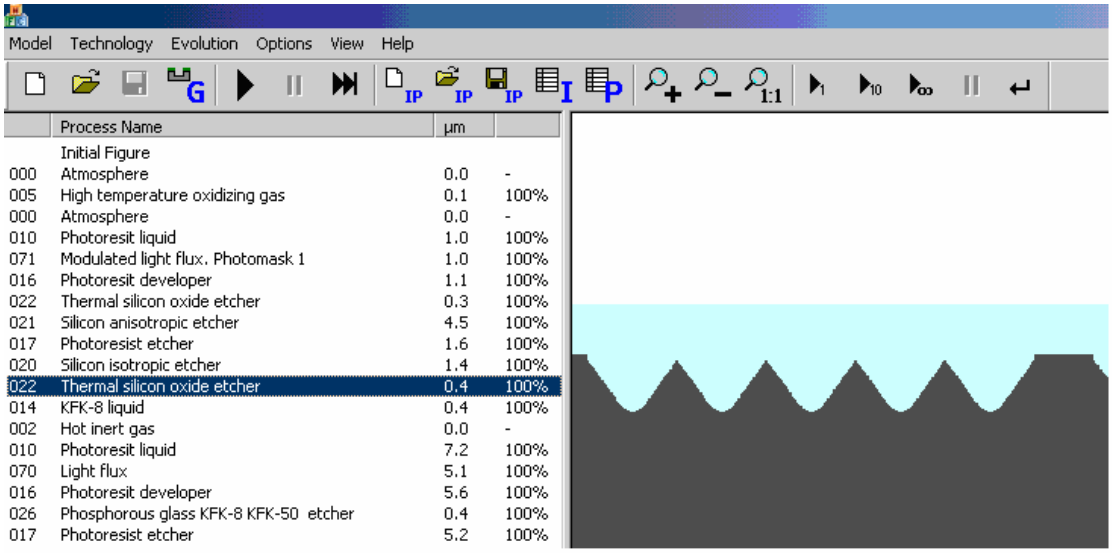

Figure 50: Simulation software interface (example view)

The input data for the application are:

- Parameters (set of materials)
- Interactions (set of technological processes)
- initial flat object of simulation (a cross-section of solar cell) and photomask structure

The output data of the application is sequence of media, obtained as a result of interactive simulations, enabling construction of desired solar cell structure. The software satisfies requirements from functional specifications and operates in MS Windows 2000/XP environment as stand-alone executable.

Task worked on	Contractor(s) involved
Develop software program for optimisation of self-formation methods	MSI

Achievements / Progress made on this task

Develop software program for optimisation of self-formation methods, in order to be able to optimise:

- selection of materials;
- patterning processes;
- manufacturing technologies.

Optimisation of self-formation methods allows selection of the optimal structure both in terms of manufacturing technology and physical characteristics of the target object. The optimisation system combines the use of both self-formation simulation software and physical characteristic simulation software. Although selection of technology in self-formation simulation depends to some extent on geometrical configuration of the target object, it is the physical characteristics simulations where geometrical configuration may have very significant impact on solar cell efficiency. Therefore optimisation software will focus on geometrical parameters of the structure obtained from self-formation simulation. The basis of physical characteristics simulation is DESSIS software from ISE TCAD software suite. The optimisation system has to perform the following tasks:

- Run self-formation simulation
- Export simulation data and convert it to for physical characteristic simulations
- Run physical characteristic simulations in a loop, by varying specified geometrical parameters.

There are two major software modules developed in REFLECTS – self-formation simulation and self-formation optimization. Both modules can be viewed as a tool for designing new solar cell technologies. The software in REFLECTS facilitates the design process and automates some tasks along the way. Another perspective would be to treat the software as some special kind of testing devices for verifying ideas of feasibility of the new technologies. If such tests are not passed, then certainly adjustments are needed for a technology to be successful.

The two software modules address different kind of problems. The self-formation simulation provides a topological simulation of technological process sequence (that is, a “routing card”). The topological simulation is not based on exact simulations of undergoing physical processes; however, it provides an accurate answer about topology (= geometrical configuration) of a new structure, in particular whether given processing steps (routing card) lead to the desired structure. Such knowledge allows to spot problems related to formation of the structure. As a result, improvements to the routing card may be identified, or a certain route may be found as technologically unsuitable.

Structure optimization software, on the other hand, is a precise electrical characteristics simulator. It has to answer which structure is better than other alternatives. *The* key performance criterion for such comparison is efficiency of the solar cell. This may seem easy, but in reality efficiency depends on many different parameters – both of geometrical configuration and of materials used.

The complete simulation space of all related parameters may just be too large to be handled by a computer system, reasonable for such a task, especially at high precision, which requires huge computational resources. Therefore, the human engineer has to direct simulation to where he believes the most probable efficiency maximum lies, by choosing clever start parameters.

In the process of technology design both software modules are used in tandem, and iteration steps both within the respective modules and interactively do exist. They give an indication whether certain technological routes are promising to further pusrsue. Finally, the decision has to be matched against existing technological facilities/possibilities, and other factors that are not accounted for in the software simulations (such as material costs, availability of resources, etc).

Software overview

The main objective of the software is optimization of patterning processes and selection of materials. Patterning processes determine the geometrical structure of the solar cell. Both geometrical structure and selected materials directly affect solar cell efficiency. In reality, there are more criteria than just efficiency in determining how good a solar cell design is, e.g., the manufacturing costs for a given technology, the repeatability of the structure, the complexity of the structure, etc. However, to keep the simulation software manageable, the theoretical efficiency of a given solar cell structure is the leading parameter to be optimised, and will serve as a basis for final decisions regarding the suitability of the technology.

The object of simulations is the ORTO solar cell structure (Figure 51). This is a solar cell with a repetitive surface pattern, consisting of vertical grooves on its surface. The emitter and base are allocated in different grooves, on the same side. It is important to notice, that different ORTO geometrical configurations can be defined by five essential parameters:

- width of emitter groove (a)
- bridge distance between emitter and base (b)
- width of base groove (c)
- groove depth (d)
- wafer thickness (D)

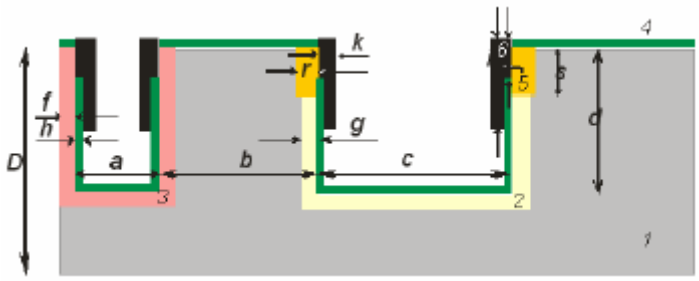

Figure 51: Schematic structure of the ORTO solar cell

The efficiency of a solar cell is influenced not only by its geometrical structure, but also by material-related physical properties – e.g., electron lifetime in silicon. Optimization software must aid in finding parameter value ranges and their combinations, which have the essential influence on solar cell efficiency. Although most likely there is an optimum for efficiency, full search or even heuristic

search of parametric space may be impossible to achieve in practice, due to the complexity of all these interacting parameters that require a huge amount of computing power which is not readily available, definitely not in SMEs. Therefore, after discussion with the SMEs, the software has been set up to provide various efficiency dependencies, based on a range of valus. It is up to the human engineer to define such value ranges, conduct sufficient simulations and finally make a decision on parameter combinations to provide a running start for the software to find the theoretical efficiency maximum. Whether simulations are "sufficient", the human engineer will decide by factoring in required accuracy, power of computer system, complexity of the structure, different characteristics of materials used, allocated time for simulations, etc. An approximation of the required computing power can be obtained from the fact that one point in a single dependency may take up from seconds to several minutes of CPU time on an average system, while dependency curves are based on 10-40 points.

Physical model

Basic semiconductor equations

In order to find the efficiency of a solar cell, it is necessary to calculate voltage-current characteristics (U I) of the solar cell. The efficiency can be calculated by the following formula:

$$\eta = \frac{U_{mp} I_{mp}}{QS};$$

where:

- U_{mp} and I_{mp} are voltage and current respectively, when output power of solar cell is maximum
- Q – incident light irradiation density, and
- S – area of the cell.

To calculate the current flowing through a solar cell, one needs to find out charge carrier or quasi-Fermi level distributions in the emitter, base and inside the pn junction. This can be achieved by solving systems of basic semiconductor equations:

Poison equation

$$\nabla \cdot \varphi = -\frac{e^-}{\varepsilon\varepsilon_0}\left(p - n + N_{D^+} - N_{A^-}\right),$$

stationary electron continuity

$$\nabla \cdot \vec{J}_n = e^-\left(R + G\right),$$

stationary hole continuity

$$-\nabla \cdot \vec{J}_p = e^-\left(R + G\right);$$

where:

- φ – electrostatic potential,
- e^- – the elementary charge,
- p and n – electron and hole densities,

- N_D+ and − N_A– densities of ionized donors and acceptors,
- R – net electron-hole recombination rate, and
- G is net electron-hole photo generation rate.

The current densities for electrons and holes are given by:

$$\vec{J}_n = -ne^- \mu_n \nabla \cdot \phi_n ,$$
$$\vec{J}_p = -pe^- \mu_p \nabla \cdot \phi_p ;$$

where:

- μ_n and μ_p – electron and hole mobility
- φ_n and φ_p – electron and hole quasi-Fermi potentials.

Electron and hole densities are connected with the electron and hole quasi-Fermi potentials, and vice versa, via well-known statistical formulas.

Since it is important to keep simulation precision for heavily doped emitters, Fermi-Dirac statistics were assumed and then the formulas read:

$$n = N_C F_{\frac{1}{2}}\left(\frac{-e^-\phi_n - E_C}{kT}\right), \qquad p = N_V F_{\frac{1}{2}}\left(\frac{E_V + e^-\phi_p}{kT}\right);$$

where:

- N_C and N_V are effective density of states,
- E_C and E_V – conduction and valence band edges,
- $F_{½}$ is the Fermi integral of order ½.

Boundary conditions

To solve the continuity and Poisson equations one needs to describe the boundary conditions. First let's describe the Fermi level boundary conditions. At the silicon-passivation layer interface:

$$\varphi = \phi_{bb} ;$$

where bb φ is the Fermi potential at the surface[14]. This potential originates from band bending which is caused by lattice discontinuity, absorption of impurity atoms and fixed charge at the surface. Similar condition can be written for silicon-metal finger interface:

$$\varphi = \phi_{bbcont} + \phi_F ;$$

where φ_F – Fermi potential at the contact.

It can be found from the following equation:

$$\vec{S} \cdot \left(\vec{J}_n(\phi_F) + \vec{J}_p(\phi_F)\right) = \frac{U_{app} - \phi_F}{R_{f+c}} ;$$

[14] A. Juodviršis, M.Mikalkevičius and S. Vengris, "Puslaidininkių fizikos pagrindai", Mokslas,1985

where app U – applied voltage at the metal finger, c f R + – the sum of finger and silicon-metal finger contact resistances.

Both for the silicon-passivation layer and for the silicon-metal finger interfaces the following current boundary conditions can be written as

$$\vec{J}_n \cdot \bar{S} = e^- v_n (n - n_0)$$
$$\vec{J}_p \cdot \bar{S} = e^- v_p (p - p_0)$$

where n v and p v are the corresponding electron and hole recombination velocities, 0 n and 0 p – the electron and hole equilibrium concentrations. Usually recombination velocity values are experimentally extracted by using Maxwell–Boltzmann statistics. There is a model for converting these values to match Fermi-Dirac statistics[15]. It is not necessary to simulate the whole solar cell, since a fragment of the cell will have the same characteristics as the whole cell. At the interception planes reflective boundary conditions are applied:

$$\vec{J}_n \cdot \bar{S} = 0$$
$$\vec{J}_p \cdot \bar{S} = 0.$$

Semiconductor models

Mobility

In doped semiconductors scattering of the carriers by charged impurity ions leads to degradation of the carrier mobility, herewith and minority carrier diffusion length. Since solar cell characteristics drastically depend on the diffusion length of minority carriers, the mobility should not be considered as a constant. One of the available models for evaluation of mobility dependence on the doping is the Masetti model[16]. Similarly, in electric fields, the carrier drift velocity is no longer proportional to the electric field strength. Instead, the velocity saturates to a finite speed. For evaluation of the mobility dependence on electric field, one of the available models is the model of Canali[17].

Recombination

There are several mechanisms of recombination in semiconductors. The most significant for solar cells are recombination through deep levels in the gap (Shockley–Read–Hall) and band-to-band recombination (Auger). The following form of SRH recombination is implemented in this model:

$$R_{SRH} = \frac{np - \gamma_n \gamma_p n_{ieff}^2}{\tau_p \left(n + \gamma_n n_{ieff}\right) + \tau_n \left(p + \gamma_p n_{ieff}\right)};$$

where coefficients

[15] Pietro P. Altermatt, Jürgen O. Schumacher, Andres Cuevas, Mark J. Kerr, Stefan W. Glunz, Richard R. King, Gernot Heiser, Andreas Schenk, „Numerical modeling of highly doped Si:P emitters based on Fermi–Dirac statistics and self-consistent material parameters“, Journal of Applied Physics, Volume 92, pp. 3187-3197, 2002

[16] G. Masetti, M. Severi, and S. Solmi, “Modeling of carrier mobility against carrier concentration in Arsenic-, Phosphorus- and Boron-doped Silicon,” IEEE Transactions on Electron Devices, Volume ED-30, pp. 764–769, 1983.

[17] C. Canali, G. Majni, R. Minder, and G. Ottaviani, “Electron and hole drift velocity measurements in Silicon and their empirical relation to electric field and temperature,” IEEE Transactions on Electron Devices, vol. ED-22, pp. 1045–1047, 1975.

$$\gamma_n = \frac{n}{N_C}\exp\left(\frac{e^-\phi_n + E_C}{kT}\right) \text{ and } \gamma_p = \frac{p}{N_V}\exp\left(-\frac{e^-\phi_p + E_V}{kT}\right),$$

n – effective intrinsic concentration, n τ and p τ – electron and hole life-times.

The effective intrinsic concentration, n_{ieff}, is expressed by

$$n_{ieff} = n_i \exp\left(\frac{\Delta E_g}{2kT}\right);$$

where n_i – intrinsic concentration, ΔE_g – band gap narrowing value.

Thus the band gap narrowing is an important calculation parameter. For precise simulations of solar cells its dependence on doping should be considered. One of available models for evaluation its dependence on doping is the Bennett model[18], where the band-gap narrowing values are extracted from experimental data assuming Maxwell–Boltzmann statistics. However, in the high-doping materials Maxwell–Boltzmann statistics differ significantly from the Fermi-Dirac statistics. Therefore, a correction must be applied to reduce the errors introduced by using Maxwell–Boltzmann statistics for the interpretation of experiments. The following form of Auger recombination is implemented in this model:

$$R_A = \left(C_n n + C_p p\right)\left(np - n_{ieff}^2\right);$$

where coefficients C_n and C_p can be taken from[19].

Thus, the net recombination which is examined in above continuity equations is

$$R = R_{SRH} + R_A.$$

Light absorption

If an active surface of the solar cell is smooth (non-textured but with one or more antireflection coatings), and an optical beam strikes the surface perpendicularly, the photo generation can be assumed as a 1D function. Let x be an axis perpendicular to solar cell surface. When the spectral irradiance per unit area at point x is

$$D_\lambda = (1 - R_\lambda) D_{0\lambda} \exp\left(-\frac{\alpha_\lambda}{x - x_0}\right) \quad \left[\frac{mW}{cm^2 \cdot nm}\right];$$

where:

- λ – wavelength,
- $D_{0\lambda}$ – incident irradiance [5],

[18] H. S. Bennett and C. L. Wilson, “Statistical Comparisons of Data on Band-Gap Narrowing in Heavily Doped Silicon: Electrical and Optical Measurements,” Journal of Applied Physics, Volume 55, pp. 3582–3587, 1984.

[19] Pietro P. Altermatt, Jan Schmidt, Gernot Heiser, and Armin G. Aberle, “Assessment and parameterisation of Coulomb-enhanced Auger recombination coefficients in lowly injected crystalline silicon”, Journal of Applied Physics, Volume 82, pp. 4711-5271, 1997.

- R_λ – reflection coefficient,
- α_λ – absorption coefficient [6],
- x_0 – the coordinate at the semiconductor surface. Assuming, that one photon, with energy higher than band gap, can generate one electron-hole pair, generation function for wavelength λ reads

$$dG_\lambda = \frac{1}{E_\lambda}\frac{dD_\lambda}{dx}d\lambda;$$

where $E_\lambda = hc$ is energy of photon of wavelength λ, h – Planck's constant, c – speed of light. The net generation function for whole solar spectrum then reads

$$G = \int_0^{\lambda_g} dG_\lambda;$$

where G_λ is a photon wavelength corresponding the energy of band gap.

Software structure

The simulation process consists of data preparation, the simulation, and result extraction. The main module SF-optimize reads input data and prepares loop parameters. Afterwards mesh and dessis are invoked in a loop sequence. Mesh puts a grid on the structure and prepares for equation solving by finite element method. Dessis iteratively solves the equations. SF-optimize reads results from dessis and adds a summary line into results_all.txt. At the end of simulation loop results_all.txt will contain summaries from all simulations. All data exchange operations are handled by SF-optimize. Input.txt is used exclusively by SF-optimize. It contains information required to build a loop. Mdr.cmd and mdr.bnd are stubs for Mesh. SF-optimize modifies those file to reflect correct dimensions of the structure beeing simulated. Likewise, des_init.cmd and dessisOx.par are modified for dessis.

Software usage

Requirements for the operating environment

The Self-formation structure optimization software runs in Windows operating system. External modules mesh.exe and dessis.exe from ISE TCAD suite have to be present and available on program path. Archiver 7-zip.exe is used for compressing result data. Simulation input data files must be placed in the current folder, where the main batch executable resides. The software runs in terminal window.

Input data

The optimization object is the geometry of ORTO solar cell structure (Figure 52). The characteristic pattern of the structure consists of vertical emitter and base grooves. Dimensions of the grooves, and distance between grooves define the solar cell configuration. Efficiency calculations require certain regions defined in solar cell structure - emitter and base profiles, passivation layers. The configuration of layers depends on groove position and dimensions. Therefore the essential parameters which distinguish one configuration from another are groove widths and depths. It is assumed that solar cell fragment is symmetrical, emitter section in the center, base section divided between left and right sides.

Input data for the software consists of the following files:

- parameter range information input.txt

- tcad dessis parameter stub files des_init.cmd and dessisOx.par

- structure definition stub files mdr.bnd and mdr.cmd

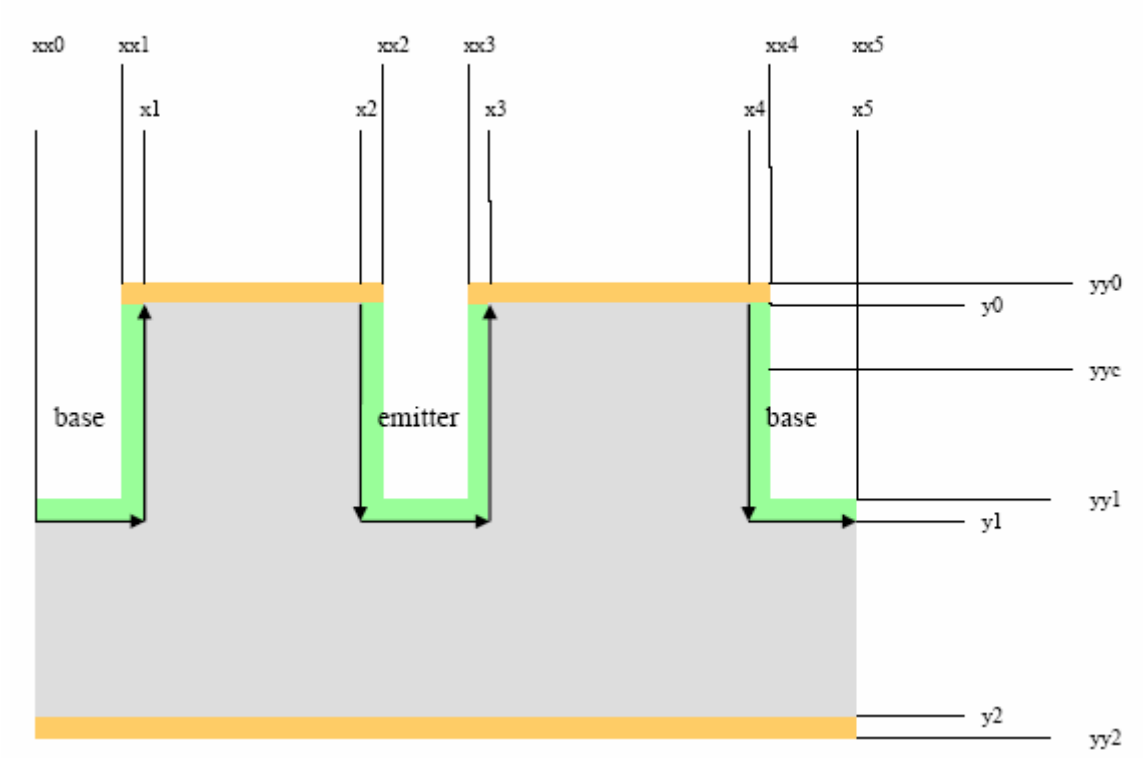

Figure 52: Parameters of ORTO structure required in simulations

Parameter range

Input.txt file defines number of simulations to run, and parameters for each simulation. Below is one possible example of such file:

```
=file start================
Simulation_1
a 20 *
c 20 *
b 20 30 40 *
d 60 *

Simulation_2
a 30 *
c 30 50 *
b 30*
d 40 60 *
*
=file end================
```

Figure 53: Example of input file

The consolidated data is plotted together, separately for different electron lifetimes (Figure 54).

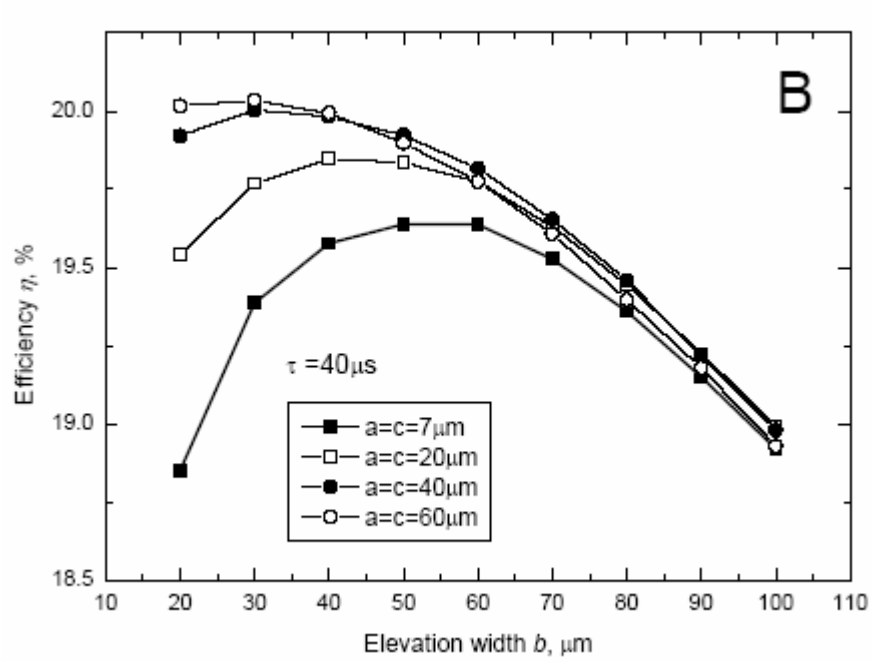

Figure 54: ORTO solar cell efficiency dependencies on the bridge width b, electron bulk lifetimes (A-C) is 40 μs

The meaning of parameters:

a – width of the base in microns,

b – width of the bridge between base and emitter,

c – width of the emitter,

d – depth of the base and emitter.

The syntax rules are as follows:

- Task name is specified in one line
- The following line must contain character a,b,c or d, followed by set of number values
- The line must be ended by asterisk (*). There must be a space between the last number and the asterisk
- The next line must contain another of (a,b,c,d) set.
- There must be 4 lines for each of (a,b,c,d)
- Another task may follow (name and a,b,c,d sets)
- When all tasks are enumerated, additional asterisk is placed at the end of the file.

The example above would generate the following parameter sequences for simulations:

- a=20 b=20 c=20 d=60
- a=20 b=30 b=20 d=60
- a=20 b=40 b=20 d=60
- a=30 b=30 c=30 d=40

- a=30 b=30 c=30 d=60
- a=30 b=30 c=50 d=40
- a=30 b=30 c=50 d=60

Tcad parameters

Tcad parameter files:

- des_init.cmd

- dessisOx.par

- mdr.bnd

- mdr.cmd

Tcad parameters consist of structure geometry files for mesh generation and parameters for equation solving. Only file stubs have to be provided. Actual input files are constructed by adding geometry parameters of particular simulation. Mdr.bnd is expected to represent a structure with parameters a, b, c, d and D. The file is expected to contain exactly 28 points. It must be presented in the format recognized by mesh. Mdr.Cmd file must contain the element refinement regions and doping profiles and locations. Des-init.cmd file describes the physical models which were used in the simulation.

dessisOx.par is a set of parameters for the models described in Des-init.cmd file.

Running simulations

To start simulation the following files must be available in a single folder:

- SF-optimize.exe

- input.txt

- mdr.bnd

- mdr.cmd

- des_init.cmd

- dessisOx.par

The simulation is started by running SF-optimize.exe in terminal window. The progress of simulations is displayed in the same window. After all tasks are completed a finish message is displayed and zip archiver is invoked to create ‘results.zip’ , where all intermediate result files are placed, in case they are needed for further analysis. At this stage the terminal window can be closed. It is not unusual if the simulation takes more than several hours, especially if total number of tasks exceeds 100.

Viewing results

In order to conveniently transfer simulation data, all essential result files are placed in ‘results.zip’, which is created in the same folder where the simulation was started. The following files and folders are created in the simulations folder:

- all_results.txt. One line from each simulation task, including simulation dimensions, physical characteristics, efficiency and simulation time
- log.txt the log of simulations. The tasks invoked, times used. Nearly identical to runtime information on terminal screen.

- task folders

Tasks are defined in input.txt. The task folder tree reflecting grouping of simulations.

All essential simulation results can be extracted from all_results.txt. If necessary, intermediate result files from particular simulation can also be analyzed. A special analysis tool fromplt.exe has been developed to be used with intermediate result files. The tool is invoked without parameters. It searches for files with plt extension in the current folder and extracts relevant data into file a.dat.

2.5 Progress on Workpackage #5 - Experimental Bifacial Solar Cell Manufacturing

2.5.1 Objectives

- Elaboration of experimental technology for manufacturing of ORTO solar cells
- Development and manufacturing of c-Si solar cells with 20% cell efficiency
- Manufacturing of functional PV system based on new solar cells

2.5.2 Progress made during the project

Task worked on	Contractor(s) involved
Elaboration of experimental technology for specimen manufacturing based on optimised method for mass production	MSI, ISFH, MILLENNIUM, TELEBALTIKA, GIRASOL

Achievements / Progress made on this task

Developing a processing sequence according the ORTO-structure suggested by ISFH requires the following key technologies:

- *Mechanical groove formation by conventional dicing saw.* The groove orientation with respect to crystal orientation had been optimised to achieve vertical flanks of the grooves after saw damage removal.
- *Angle for evaporation of Al:* The angle between metal source and vertical flank of the groove has been optimised aiming at the most wide fingers at the given groove width of 50µm for the narrow grooves.

The ISFH-ORTO cell suggested to the project partners by ISFH was first realised in the last reporting period. The applied key technologies are:

Mechanical groove formation by conventional dicing saw.

- The groove orientation with respect to crystal orientation had been optimised to achieve vertical flanks of the grooves after saw damage removal. Figure 55 shows the grooves

aligned 30° to the flat. Here the etching with KOH-solution gives the desired rectangular shape of the grooves. The vertical flanks are necessary for a proper metallization.

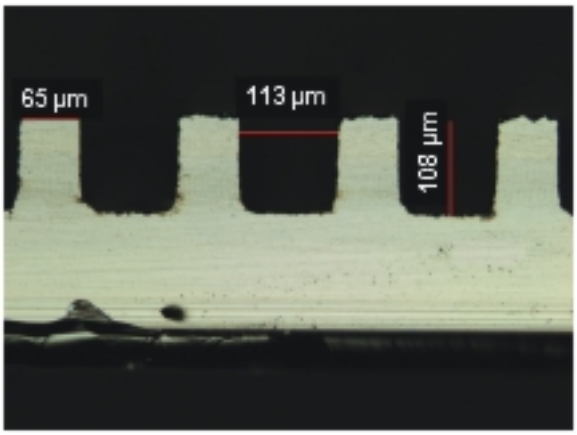

Figure 55: Optimisation of groove formation with regard to obtaining rectangular grooves.

Shallow angle evaporation of Al:

- The angle between metal source and vertical flank of the groove has been optimised aiming at the widest fingers at the given groove width of 70 µm for the narrow grooves.

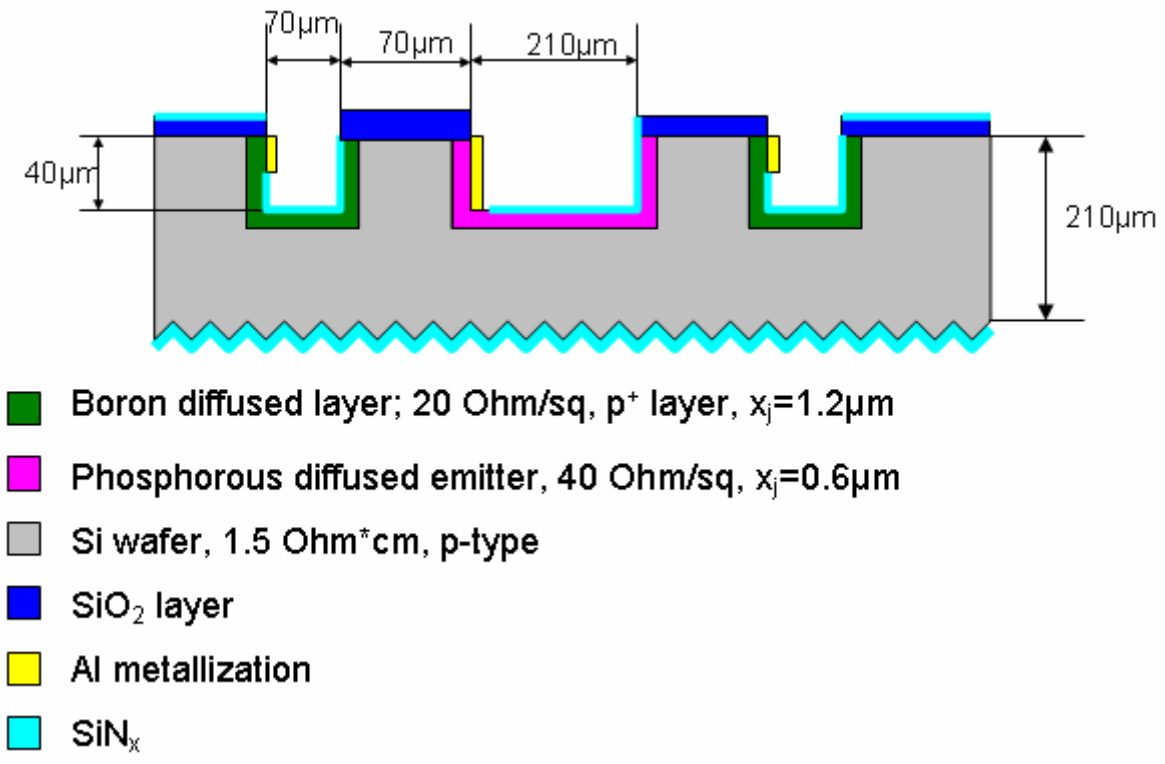

Figure 56: Schematic of the geometry of the ISFH-ORTO Cell

Task worked on	Contractor(s) involved
Manufacture of experimental specimens of bifacial solar cells according to new solar cell production protocol	MSI. ISFH, TELEBALTIKA, MILLENNIUM, GIRASOL,

Achievements / Progress made on this task

Based on the ISFH-ORTO-solar cell design suggested by ISFH (WP3), which leads to a simplification of the processing sequence further process optimisations have been carried out. The focus of this optimisation was the adjustment of the individual processing step to each other aiming at better process control and higher efficiencies. The processing sequence is listed below.

- Thermal oxidation
- SiN deposition on both sides
- ***Cutting the base contact grooves with dicing saw***
- Saw damage etch
- Removal of SiN
- B-Diffusion + Removal of Boron glass and skin
- SiN deposition on both sides
- ***Cutting the emitter contact grooves with dicing saw***
- Saw damage etch
- P-Diffusion + P-glass removal
- SiN removal
- RS SiN deposition
- FS SiO_2 removal
- Texturing
- RS SiN removal
- FS SiN deposition
- ***Shallow angle finger evaporation: OECO-principle***
- Busbar evaporation
- RS SiN for passivation

The major differences compared to the process suggested formerly are the following:

- High temperature processes: only one thermal oxidation process is needed instead of four
- Photolithography: no photolithography at all is needed instead of three steps for each cell side. This is a huge cost savings.
- Vacuum deposition of metals: only one deposition has to be carried out for contract fingers of both polarities. The additional evaporation of the busbars can be omitted by replacing this step using e. g. conductive adhesives.
- Surface passivation. All surfaces are passivated.

- Large contact area. The contact area is now restricted to the lowest possible level.
- Shading losses. Cells are illuminated from the non-metallised front side, hence shading doesn't take place. The shading on the rear side of the bifacial cell is minimised due to the OECO-contact principle.

ORTO solar cell results

After optimisation in particular of the contact geometry and the base resistivity the short circuit current was significantly enhanced. The best cell efficiency with the above mentioned cell design was 20.5 % on aperture area of 3.9 cm^2. Thus the project aim is achieved. In Table 6 the new and the former results are shown. The most obvious difference is the high current density of 41.1 mA/cm2 instead of about 35 mA/cm^2. The main reason for this increase is on the lower base doping resulting in a specific base resistivity of 3-4 Ω.cm. The deeper grooves for the emitter leading to a higher collection probability supporting the increase in short circuit current.

Table 6: ISFH-ORTO cell results. The highest efficiency obtained so far is 20.5 %. Thus the project aim is achieved. The cell is in this case illuminated from the non metallised side.

Illumination (aperture)	V_{OC} [mV]	J_{SC} [mA/cm^2]	*FF* [%]	Efficiency [%]
Unmetalised FS	637	41.1	78.3	**20.5**
OECO-metalised RS	630	34.8	77.5	17.0
Unmetalised FS	639	*34.3*	77.6	17.0
OECO-metalised RS	635	33.2	76.9	16.2

In Figure 57 a photograph illustrates the ISFH-ORTO cell from the non metallised and the metallised side.

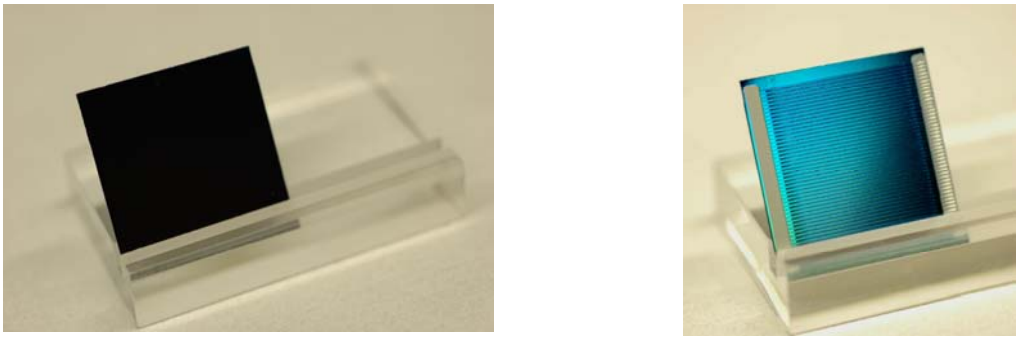

a) b)

Figure 57: Photography of an ISFH-ORTO cell from the non metallised side (a) and the metallised side (b).

Task worked on	Contractor(s) involved
Manufacturing of functional PV system based on new solar cells	MSI, ISFH, TELEBALTIKA, SAULES ENERGIJA,. CRES

Achievements / Progress made on this task

Standard ORTO module fabrication

ISFH-ORTO cells with similar short circuit current are interconnected to modules by ISFH. Five cells are connected in series. The busbars are lying at the end of the individual cells. Thus the base busbar of one cell and the emitter busbar of the adjacent cell are interconnected by a metal inter connector. Figure 58 shows a schematic of the interconnection scheme.

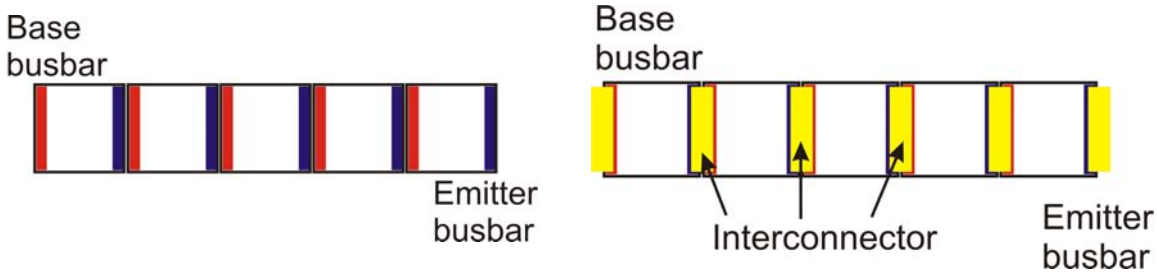

Figure 58: Schematic of the ISFH-ORTO cell interconnection. Left: positioning of the cells. Right: position of the soldered interconnector.

Figure 59 shows a photograph of the interconnector soldered to an ISFH-ORTO cell. The patterning of the interconnector allows a certain mechanical flexibility in the module. Since the thermal expansion coefficients of the different materials in the module are leading to a movement of the cells with versus each other and the encapsulant.

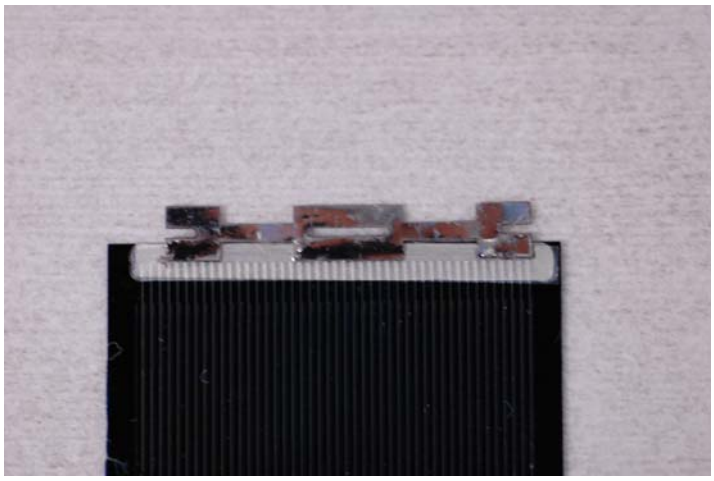

Figure 59: Interconnector used for ISFH-ORTO cell interconnection.

The first series interconnected string of ISFH-ORTO solar cells has an efficiency of above 10 % illuminated from the non metallised cell side. The efficiency of the encapsulated cells in a standard composition with a transparent tedlar at the metallised module side is about 9 %. Table 7

summarizes these results. The efficiency losses of those ISFH-ORTO cells interconnected compared to the efficiencies of the individual cells before interconnection are caused by the non optimised soldering process. The decrease can be seen in all cell parameters.

Table 7: ISFH-ORTO module results of 5 cells interconnected to a string before and after encapsulation.

	Illumination (full area)	V_{OC} [mV]	J_{SC} [mA/cm^2]	*FF* [%]	Efficiency [%]
5 cells string	Unmetallised FS	2972	20.0	69.2	10.1
	OECO-metallised RS	3036	19.8	70.1	8.4
5 cells module*	Unmetalised FS	3079	23.6	68.5	8.9
	OECO-metalised RS	3036	21.9	68.8	8.4

* 1 cell broke between measurement of the string and encapsulation. The current density is corrected for the area loss.

Fabrication of ISFH-ORTO module with reflector

The development of the reflector for the ISFH-ORTO module is described in WP2 and deliverable D4 (D2.1). The calculations were carried out by ISFH and the manufacturing by the project partner Optical Products. A string consisting of 5 ISFH-ORTO cells was conventionally laminated to the reflector. The front side is only covered by EVA (Ethyl Venyl Acetate) film, no glass is laminated to the module. Tests regarding the mechanical stability of the acrylic at a temperature of 150°C have been conducted using a cubic 5 x 5 cm^2 piece of acrylic with a thickness of about 1 cm. This acrylic did not deform during lamination. The reflector, however, was less stable due to its particular shape. In Figure 60 the yellow lines illustrates where the curvature is missing and instead the acrylic is flat here. The consequence of this deformation was that the Al metal layer on the rear of the reflector got cracks.

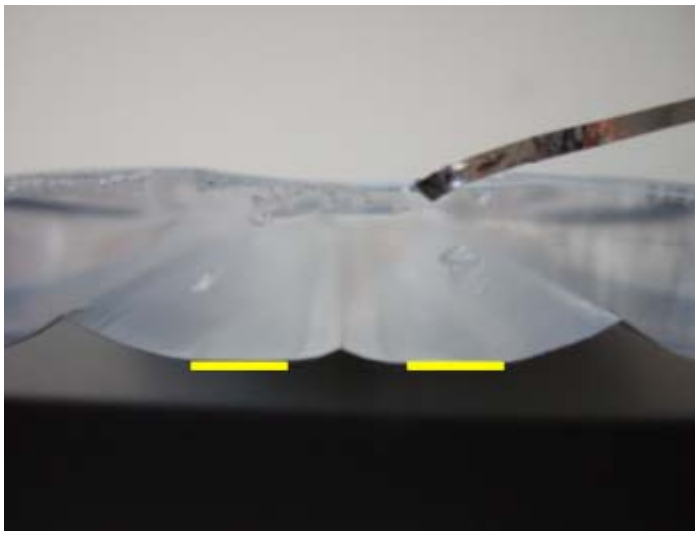

Figure 60: Cross section of the reflector with encapsulant. The deformed part of the reflector is marked in yellow.

Despite these difficult circumstances the reflector works well as can be seen in Figure 61 from the mirror image. Here the rear of the cells are reflected.

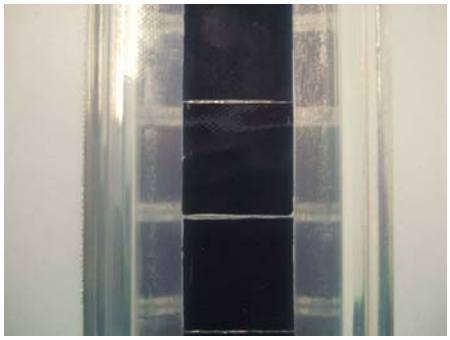

Figure 61: ISFH-ORTO cell string. Two mirror images are visible on the right and on the left from the string in the middle.

The electrical measurements of the module are carried out by our project partner CRES in Athens. **Error! Reference source not found.** demonstrates the whole ISFH-ORTO module with reflector.

2.6 Progress on Workpackage #6 - Bench Tests, Laboratory Testing and Evaluations

2.6.1 Objectives

Testing the REFLECTS prototypes with respect to their performance specification, stability, reproduceability, etc.

2.6.2 Progress made during the project

Task worked on	Contractor(s) involved
Testing the performance of the novel bifacial cell and the reflector performance	CRES, GIRASOL

Achievements / Progress made on this task

Testing subtasks were defined as:

– achieved efficiency

– life

– reliability and stability under different conditions

– sensitivity to duty cycle

– reproduceability,

– reflector specular reflectance

– reflector temperature sensitivity

– reflector stability

Solar cell and sub-module electrical characteristics testing

The characterization of solar cells and modules plays a decisive role in many activities including quality control, the evaluation of manufacturers' guarantees and the dimensioning of solar systems. In current practice the photovoltaic performance of a solar device is determined by exposing it at a known temperature to stable sunlight, natural or simulated and tracing its current-voltage characteristic while measuring the magnitude of the incident irradiance. The measured performance is then corrected to Standard Test Conditions (STC) or other desired conditions of irradiance and temperature. The corrected power output at the rated voltage and STC is commonly referred to as the rated power. The solar devices have a wavelength dependent response and their performance is significantly affected by the spectral distribution of the incident radiation, which in natural sunlight varies with the location, weather, season of the year and day of year. As for simulated sunlight it varies with the type of the solar simulator and the testing conditions.

Solar cell tester

A solar cell tester made by Spectra-Nova's, model S-N CTA 100 Class A Solar Simulator was used for testing (Figure 62). It was originally designed to be used in production and development environment for solar photovoltaic cells.

The solar cell tester is composed of:

graphical user interface and parameter fitting package

electronic load

light generator

test and measurement unit

c-Si reference cell

The solar radiation is measured by a reference c-Si cell mounted permanently at the side of the chuck. The reference cell is kept at a constant temperature of 25°C by a Peltier device. The reference cell was calibrated with respect to a portable first class reference c-Si cell placed at the surface of the chuck. The solar cell tester complies with the standard IEC 60904-9. It uses a continuous wave light (Xenon lamp) with appropriate filter. The radiation spectrum complies with the air mass AM1.5 (Air Mass 1.5) standard.

The test setup is as follows:

- four-probe contacting technique
- •vacuum hold chuck (copper base) for single solar cells
- multiple contacting probes
- electronic load
- data acquisition equipment

The measurements on the sub-module prototypes provided were performed using the four-probe technique by connecting the sub-module output wires to the appropriate input points. Full I-V curves were taken with 100 data points per curve at solar radiations ranging between 680 and 1060 W/m^2. The sample temperature was measured by inserting a thermocouple under the prototype sub-module making sure that it makes good thermal contact. The estimated sample temperature accuracy achieved was ± 2°C. The software used for visualization and solar cell parameter fitting was provided by Spectra-Nova.

Figure 62: View of the solar cell tester at CRES PV laboratory

Measurement principles

The standard IEC 904-3 shall be followed in determining the characteristics of the solar cells and modules. The principles in this standard are designed to reduce discrepancies by relating the performance rating to a reference terrestrial solar spectral irradiance distribution. This is done by measuring the irradiance with a reference device that has essentially the same relative response as the test specimen and has been calibrated in terms of short-circuit current per unit of irradiance area with the reference spectral distribution. In order to obtain a Current-Voltage (I-V) curve for a given specimen we need at least 100 samples of measurements. The values are corrected for Standard Temperature (25°C) and targeted irradiance. A standard full sweep of current and voltage for 100 measurement points takes about 3 seconds.

A temperature sensor (J-type thermocouple) is used to measure the cell or sub-module temperature during the tests. The realized temperature accuracy is estimated to be within ±2°C.

Reference solar cells or modules are used to correct for spectral mismatch. If the reference is of the same construction and type as the measured module, the error in the determined power value is ± 2.5% (precision measurement). If a standard reference is used (similar to the measured module or cell), the error increases to a maximum of ±5% (standard measurement).

Task worked on	Contractor(s) involved
Testing the performance of a prototype system (module + reflector).	CRES, GIRASOL

Achievements / Progress made on this task

Test procedures include

– Thermal tests (thermal cycling, damp heat,…)

– Mechanical stress tests

– Electrical tests (Insulation, hot-spot,…)

– Exposure tests (UV, outdoor,…)

The standards for c-Si PV module certification that were used is IEC 61215 (titled : Crystalline Silicon Terrestrial Photovoltaic (PV) Modules - Qualification and Type-approval).

5 cells in series encapsulated on glass

CRES received a sub-module of size 14 cm by 14 cm, it was composed of 5 cells of dimension 2.45 cm by 2.45 cm, for a total solar cell area of the module of 30.01 cm^2. One of the cells was chipped and approximately 0.8 cm^2 of cell is missing. The effective total solar cell area was 29.21 cm^2. The sub-module prototype is presented in Figure 63. All 5 cells were connected in series. The cells were encapsulated at the back of a piece of solar glass encapsulated in silicon resin backed with transparent Tedlar. Two flat wires were coming out of the laminate to be used for electrical connection.

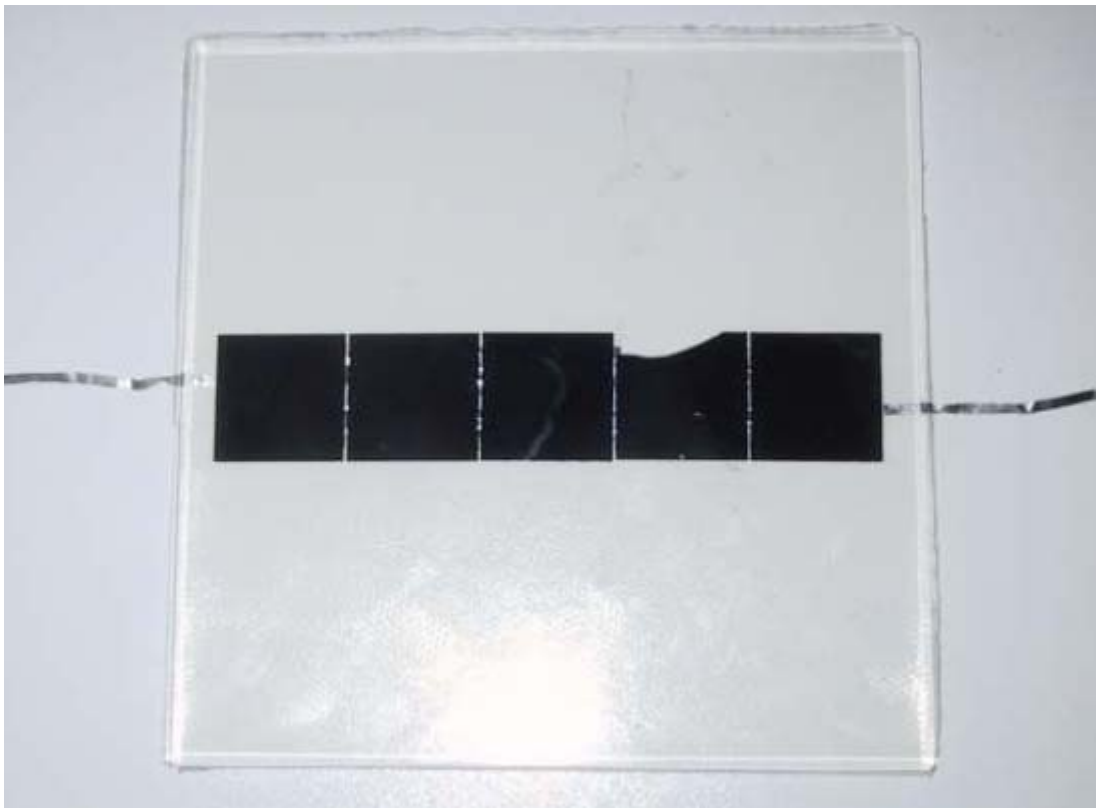

Figure 63: The solar cell sub-module encapsulated at the back of solar glass provided to CRES by ISFH

A couple of very small drops of lead solder were observed on two cells, but these were not considered to have any significant bearing to the results.

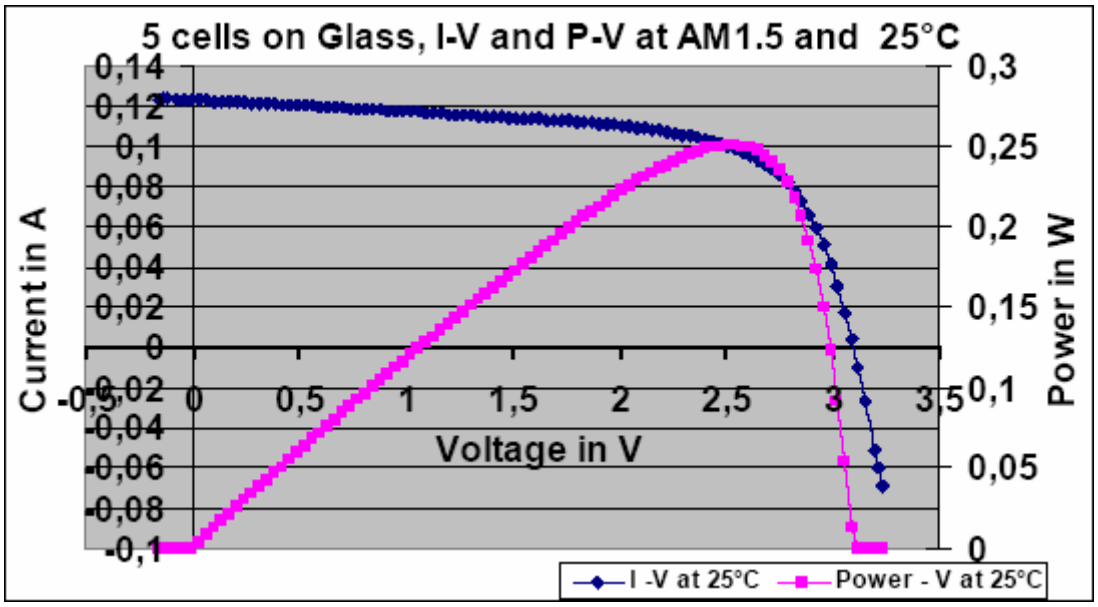

Figure 64: I-V and P-V curves at AM 1.5, 1000W/m2 and 25°C of the sub-module referred as 5 cells on glass prepared by ISFH

Below you can find the measured and calculated parameters:

Module physical parameters and testing conditions:

- Individual solar cell size: 2.45 by 2.45 cm^2 (±0.05cm)
- Number of cells in connected in series: 5
- Number of cells connected in parallel: 1
- Total solar cell area: 29.21 cm^2 (±2%)
- Temperature of reference cell: 25 °C ± 1°C
- Temperature of sub-module: 38 °C ± 2°C
- Illumination intensity: 1010 W/ cm^2 ± 2%

The I-V curve was taken at the above mentioned conditions and was converted to 25°C and 1000 W/m^2 at AM1.5. The variation of voltage and current with the temperature was deduced experimentally by I-V curves taken at two different temperatures. IV/IT was calculated to be - 4 mV per °C and II/IT was calculated to be 0.3 mA per °C.

Calculated sub-module parameters:

- Maximum power (Pmp): 0.250 W
- Voltage at max. power (Vmp): 2.542 V
- Current at max. power (Imp): 0.0985A
- Voltage at open circuit (Voc): 3.082 V
- Current at short circuit (Isc): 0.123 A
- Current density at short circuit: 4.21 mA/cm^2
- Fill factor: 66.09 %
- Cell efficiency: 8.495 %
- Series resistance: 3.549 K
- Shunt resistance: 186.93 K

Given the accuracy of the measured parameters and the earlier error discussion, it is concluded that the accuracy of the above calculated parameters is considered to be within ±5%.

5 cells in series encapsulated on an acrylic reflector

CRES received a sub-module of size 30.7 cm by 6.8 cm by 1.55 cm maximum thickness. It was composed of 5 cells of dimension 2.45 cm by 2.45 cm, for a total solar cell area of the sub-module of 30 cm^2. The module is presented in Figure 65. All 5 cells were connected in series. The cells were encapsulated in a groove on top of a transparent acrylic reflector and were covered with silicon resin and EVA. Two flat wires were coming out of the laminate to be used for electrical connection.

Figure 65: The solar-cell submodule with acrylic reflector provided by ISFH to CRES

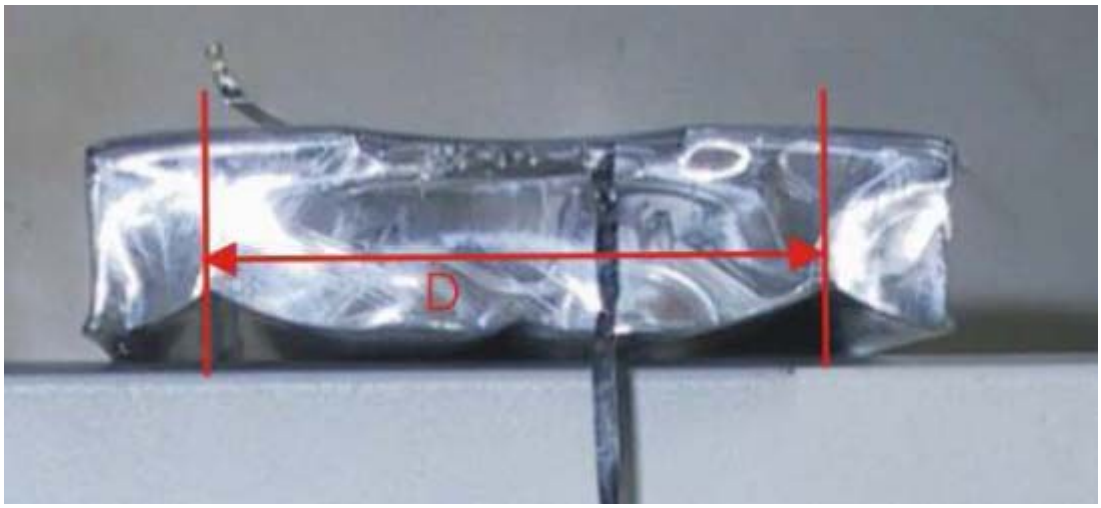

Figure 66: Profile of acrylic reflector with a groove distinguished on the top, where the solar cells were inserted. D is the width considered when the efficiency of the sub-module is calculated.

The reflector was designed to be installed at for a fixed support structure. The normal to the cells surface is considered pointing at the sky equator and the reflector optics were optimized for the sun's movement for a whole year.

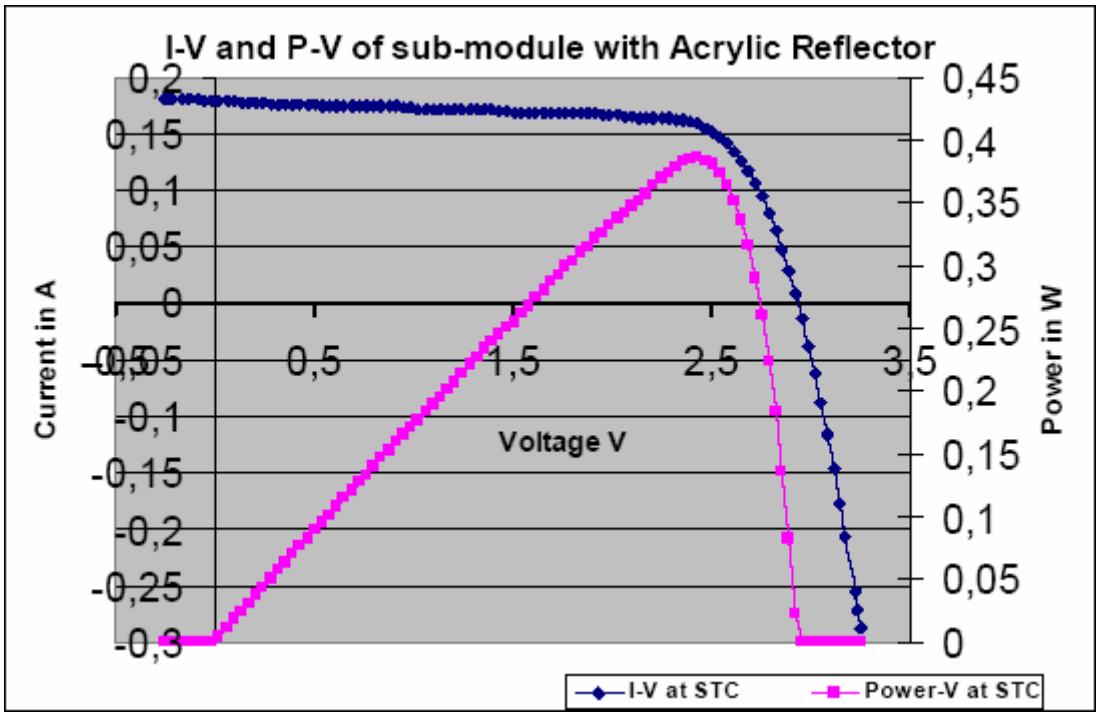

Figure 67: I-V and P-V curves at AM1.5, 1000W/m2 and 25°C of the solar cell string mounted on the sub-module referred as 5 cells encapsulated on top of acrylic reflector prepared by ISFH

Below you can find the measured and calculated parameters:

Module physical parameters and testing conditions:

- Individual solar cell size: 2.45 by 2.45 cm^2 (±0.05 cm)
- Number of cells in connected in series: 5
- Number of cells connected in parallel: 1
- Total solar cell area: 30 cm^2 (±2%)
- Temperature of reference cell: 25 °C ± 1°C
- Temperature of sub-module: 26 °C ± 2°C
- Illumination intensity: 965 W/ cm^2 ± 2%

The I-V curve was taken at the above mentioned conditions and was converted to 25°C and 1000 W/m2 at AM1.5.

Calculated parameters of solar cell string with acrylic reflector:

- Maximum power (Pmp): 0.387 W
- Voltage at max. power (Vmp): 2.433 V
- Current at max. power (Imp): 0.159 A
- Voltage at open circuit (Voc): 2.925 V
- Current at short circuit (Isc): 0.180 A

- Current density at short circuit: 6 mA/cm2
- Fill factor: 73.49 %
- Cell efficiency: 13.366 %
- Series resistance: 1.605 K
- Shunt resistance: 186.90 K

Given the accuracy of the measured parameters and the earlier error discussion, it is concluded that the accuracy of the above calculated parameters is considered to be within ±5%.

The 5 solar cell string was measured to have an efficiency of 13.36% at STC. The sub-module efficiency taking into account the surface area of the reflector for the length of the string (solar cell string length L=12.55cm) and the width D=4.9cm (Figure 66), was calculated to be 6.16% at STC. The effective surface area LxD of the sub-module with the reflector is equal to 61.495 cm^2, about 2.04983 times larger than the actual solar cell area. The sub-module optics were not as good as anticipated since during encapsulation the reflector deformed. The absolute current at maximum powerpoint (MPP) was 159mA with the reflector compared to 98.5 mA without it (Glass encapsulated string of cells), showing that the reflector works relatively well. Under ideal conditions the current would be doubled but this is not observed. The current at MPP of the 5 solar cell string is increased by 1.614 times, when the effective surface area of the sub-module, considering the active part of the reflector surface, increases by 2.0498 times.

Conclusions

The sub-modules prepared by ISFH were measured with a solar cell tester and exhibited at STC an efficiency of about 8.5% for the glass encapsulated string and 13.36% for the acrylic reflector sub-module. The sub-module series resistance with the reflector is considered to be too high. R_{series} was calculated to be about 1.6 K for the 5 cell string or about 0.32 K per solar cell, whereas for regular mono-crystalline Si solar cells the R_{series} usually is of the order of 0.01 K. Also the acrylic reflector was deformed during the encapsulation process and secondly the aluminum film at the back of the reflector, as observed by inspection was cracked and presented gaps. Also the illumination from the solar cell tester is not perpendicular to the sample at every point. Consequently, the optical concentration and reflection did not function as designed and therefore the sub-module performed was worst than expected. Given the above comments and observations there is room for improvement and in any case the active area of solar cells is replaced with acrylic material acting as a reflector and mechanical support device of the solar cells. Finally, despite the deformed reflector we still got a current at MPP about 1.6 times higher than the 5 solar cell string encapsulated on glass.

2.7 Progress on Workpackage #7 - System Integration and Field Evaluations

2.7.1 Objectives

- Demonstrate and test system under real life conditions.
- Verifiy that researched concepts indeed work as expected/predicted in practice.

2.7.2 Progress made during the project

Based on standards for the monitoring and evaluation of photovoltaic systems developed by both the International Electrotechnical Commission (IEC) and the Institute of Electrical and Electronic Engineers, Inc (IEEE) (see the Literature at the end of the document) this document is meant to be a for data measurements for a specific PV system aiming to evaluate the performance of a prototype PV module developed in the REFLECTS project.

This specification describes in a comprehensive manner the data acquisition equipment installed in PV system and the measurements to be made. It also indicates the information to be stored by the data acquisition system. The scope of this work is to evaluate the performance of the PV module developed during the project REFLECTS and not the performance of the complete PV system. A complete PV system is required in order that the PV module encounters the appropriate operation environment for evaluation.

The following assumptions have been made. The prototype PV module will be made of approximately 30 to 36 solar cells allowing the operation with a 12 VDC battery. Should prototype limitations prohibit a PV module to be composed of 30 to 36 solar cells, two modules could be assembled with half the regular number of solar cells and connected in series, to obtain the required DC voltage. During the first technical meeting at ISFH in Hameln/Emmerthal, in January 2006 it was presented that the Si solar cells will have 2.5 x 2.5 cm dimensions, and will produce at 1 Sun approximately a short circuit current of 220-250 mA and an open circuit voltage of 0.67-0.68V. Given the relatively low power characteristics of the prototype module, to the best of our knowledge no maximum power point tracker (MPPT) or PV inverter that incorporates an MPPT is commercially available. Considering the above characteristics of the prototype PV module, the following PV standalone, DC system powering a small load like a lamp is defined.

Definition of stand alone PV system and monitoring equipment

Here are the proposed equipment composing the PV and monitoring system. All the equipment except the PV module will be commercially available devices.

- PV module (provided by REFLECTS project)
- Battery charge controller
- Battery
- Monitoring equipment
- Load

In order to be able to collect the maximum amount of energy from the PV module, the battery size and load have to be sized appropriately for the insolation (solar radiation) conditions of the

installation site so that the battery charge controller never limits the delivery of energy from the PV module to the battery. The voltage and current measurements will be used to calculate the Energy produced by the PV module.

Badham farm is the installation site in the U.K. Below we present the average insolation (10 year average) kWh/m^2/day of the London area and we assume that the Badham farm area will not be far from these values.

Table 8: Ten year average monthly insolation for the London area U.K.

Country/ City	Jan	Feb	Mar	Apr	May	Jun	Jul	Aug	Sep	Oct	Nov	Dec	Year Avg
U.K./ London	0.67	1.26	2.22	3.48	4.54	4.51	4.74	4.01	2.86	1.65	0.89	0.52	**2.61**

Table 9 below presents the specifications of the various devices that composed the studied PV system.

Table 9: Specifications of PV system periphery equipment

Device	Specifications
Battery charge controller	12 VDC nominal operation, maximum battery current to a load less than 1 A. Maximum current from the PV module is less than 500 mA. • voltage regulation • fuse • manual load switch • State of Charge indication • Low voltage disconnect • automatic load reconnection • temperature compensation • field adjustable parameters • timer for load
Battery	Lead acid, 12VDC nominal, 5 to 10 Ahr.
Load	12 VDC fluorescent lamp with 5 to 7 W consumption. The timer must be set for 0.5 to 1 Hour operation per day.

Since voltage drop can be a problem when low voltage DC devices are connected over long power cables, care should be taken in the location of DC voltage measurements. In Figure 68 the block diagram of the PV system is presented along with the points were the measurements will be made.

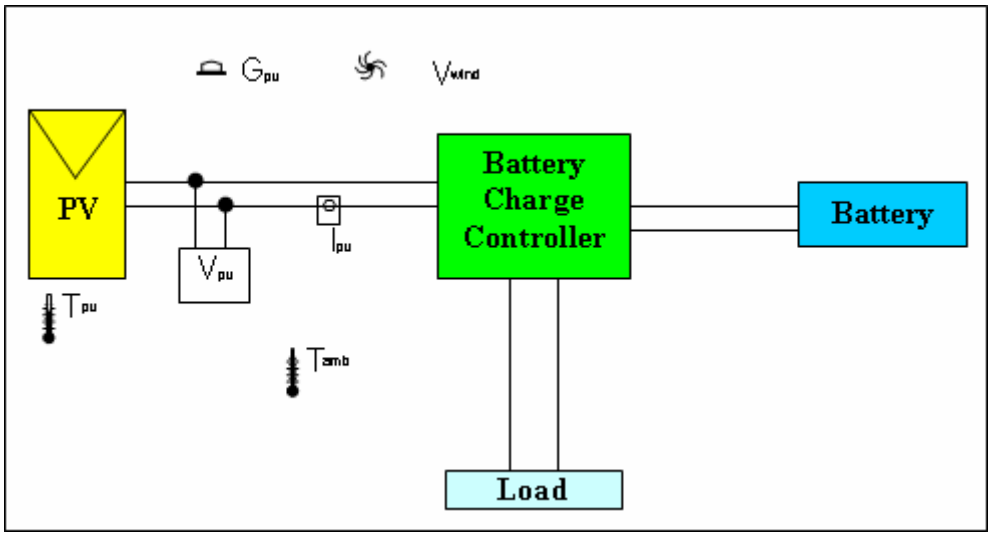

Figure 68: Block diagram of PV system requirements

Measured parameters

V_{pv} : dc voltage across the terminals of the PV module.

I_{pv} : current from the PV module before the charge controller or maximum power point tracker.

G_{pv} : Solar irradiance incident on the PV module plane of the system being measured, in W/m^2

V_{wind} : Wind velocity (m/s). The measurement should represent air flow over the PV module.

T_{pv} : The temperature sensor should be mounted at the back of the PV module making good contact with one of the Si cells.

T_{amb} : Ambient temperature (C). Sensor should be enclosed in an appropriate ventilated radiation shield mounted in a location that will indicate the environment in which the system is operating.

Signal collection and recording

Data collection can be distinguished into two different time intervals, the first is the measurement interval while the second is the storage interval. The measurement interval represents how often a sensor is used to record the value or condition it was designed to sense, such as voltage or wind speed. These measurements occur quite frequently and in most remote systems it would be impossible to record all of this information over a long period. To reduce the amount of data measurements are usually taken at a higher rate and then they are processed to provide a meaningful value over a longer time period, usually between in minutes to one hour. This is the record interval. The measurements are being continuously taken, processed and then discarded, but the important information is recorded in the data logger memory for future use.

The following sections provide information on both the collection and processing of information in the monitoring system.

Sensor measurement interval

The sensor measurements account for the majority of data collection complexity. Initially it is important to understand the dynamics of the signals being measured to insure that the information being collected is valid, meaning that it represents the phenomenon being measured. It is

important that the sample or measurement interval accurately captures the phenomena in question. Table 10 presents data collection parameters such as the frequency of collection and general information specific to the collection of such data. Collection accuracy will depend on the level and type of monitoring that will be required by the system or the desired results.

Table 10: Measured parameter specifics

Measurements		Frequency	Processing	Minimum Accuracy
V	dc voltage measurements	1 or 0.1 Hz	Average	1.0%
I	dc current measurements	1 or 0.1 Hz	Average	1.0%
Gpv	Solar irradiance on module surface	1 or 0.1 Hz	Average	5%
V_{Wind}	Wind Speed at PV module level	1min to 0.1 Hz	Average	1 m/s
Tpv	PV module temperature	1min to 0.1 Hz	Average	1 °C
T_{amb}	Ambient temperature	1min to 0.1 Hz	Average	1°C

Data recording interval

The evaluation scope of monitoring dictates the requirements for the different time intervals for data recording. For the evaluation of the prototype PV module the data collection should be based on sample rates as described in Table 11.

Table 11: Measuring and recording intervals

Measured parameters		Measuring interval	Recording interval
I_{pv}	dc current measurements	1 second	10 minutes
V_{pv}	dc voltage measurements	1 second	10 minutes
G_{pv}	Solar Radiation on array surface	1 second	10 minutes
V_{wind}	Wind Speed at site	1 Minute	10 minutes
T_{pv}	PV module temperature	1 Minute	10 minutes
T_{amb}	Ambient temperature	1 Minute	10 minutes
Calculated Parameter			
P_{pv}	Power output of PV module	1 second	10 minutes

Data acquisition system

The data acquisition system will be provided for the evaluation period by CRES, which will be responsible also for data collection and analysis. The data acquisition system requires a source of 230VAC at 50 Hz and for communication purposes a telephone line to be able to remotely connect to the logger and check the state of operation, edit the data collection program and upload data.

2.8 Progress on Workpackage #8 - Dissemination and Exploitation

2.8.1 Objectives

- To ensure that the achievements are made known to the targeted potential clients / market segments.
- To prepare plans for future exploitation to ensure that the results are implemented in real-world applications.

2.8.2 Progress made during the project

A policy of wide dissemination of project results has been pursued in particular focused on potential end users of the project results.

Task worked on	Contractor(s) involved
Set-up and maintenance of a project website	ALL

Achievements / Progress made on this task

A website has been set-up and maintained. For details, see description in 3.2 REFLECTS Web Site, Page 99.

Task worked on	Contractor(s) involved
Other dissemination activities	

Achievements / Progress made on this task

Dissemination of information to the networks and established distribution channels of the individual partners is executed on an ongoing basis. For details, see the Plan for Using and Dissemination of Knowledge in Annex A, Page 93.

2.9 Deviations from the project workplan

Problems encountered	Corrective actions taken/proposed	Contractor(s) involved
Efficiency definition in DoW not consistent with definition in PV industry	After discussions during the 6M meeting the definition as used in the PV industry for bifacial cells have been adopted.	MSI / ISFH

2.10 List of deliverables

Deliv. Nr	Deliverable name	WP#	Date due	Actual/ Forecast delivery date	Lead contractor
D1	Functional specifications for software	1	3	3	MSI
D2	Functional specifications for self-formation	1	3	3	MSI
D3	Functional specifications for reflector	1	3	3	OP
D4	Reflector Design	2	6	13	MILLENIUM
D5	Reflector Prototype	2	6	14	OP
D6	Optimal solar cell ORTO structure	3	8	8	MSI
D7	Prototype production protocol	3	12	12	ISFH
D8	Photomask engineering design	3	10	10	ISFH
D9	System Architecture Design	4	6	6	MSI
D10	Software program for simulation of self-formation	4	10	12	MSI
D11	Software program for optimisation of self-formation	4	14	14	MSI
D12	Experimental bifacial c-Si solar cells with 26% (or better) cell efficiency	5	13	13	ISFH
D13	Production protocol (routing card)	5	13	13	MSI

D14	Evaluation report on new manufacturing method	5	15	15	TELEBALTIKA
D15	PV system with new solar cells	5	15	15	SALES ENERGIJA
D16	Report describing solar cell + module performance	6	12	15	CRES
D17	Report on economical evaluation	6	22	22	GIRASOL
D18	Field test and end-user survey data	7	18	18	MILLENNIUM
D19	Report on field test results	7	24	24	MILLENNIUM
D20	Website	8	6-24	6-24	MSI
D21	Application Notes	8	24	24	MSI
D22	Publications	8	24	24	ISFH
D23	Plan for Exploitation and Use of Knowledge	8	24	24	GIRASOL
D24	Exploitation Agreement	9	24	24	GIRASOL

SECTION 3 Consortium management

3.1 Progress on Workpackage #9 – Consortium Management

3.1.1 Objectives

To ensure a smooth project management and communication

3.1.2 Progress made during the project

The project is managed by a Project Management Team, chaired by Millennium. PSU is responsible for supervision of the work programme, communication with the Commission, reporting, delegation of workpackages, motivation of the team, encouragement of creativity, correct problem solving procedures, and corrective actions. PSU also acts as project co-ordinator for day-to-day project issues. To this end they have set up and maintained a Management Office which functions as a Project Secretariat for the REFLECTS project.

The Project Management Team has organised a meeting every 6 months to review the technical progress made by each partner, and to agree in detail the actions for the next period. In addition to the formal six-monthly meetings, the partners also set up a number of working parties to ensure delivery of specific tasks, based around the partners committed to specific tasks and objectives within the work programme.

The structure for monitoring and reporting progress consists of a series of reports and meetings.

Progress of each task is assessed quarterly to ensure that there is no - or limited - deviation from the original plan and to closely control the development activities of the partners.

3.2 Consortium performance

3.2.1 General

The management and co-ordination of the REFLECTS project activities have been implemented without major problems.

3.2.2 Meetings and communication

Discussions at the meetings have been open and constructive, enabling the direction and content of the technical work to be defined and agreed. Also outside of these meetings, communication among the consortium members has been good, mainly by e-mail/phone, enabling workpackages to progress smoothly.

3.3 Contractors

3.3.1 Updated list of contractors

No changes in the project partner companies have occurred during the project.

Name	Company	@	☎
Ami ELAZARI	MILLENNIUM T.O.U.	milelec1@nonstop.net.il;	+972-9-9588071
Wieland KOORNSTRA	GIRASOL	wkoornstra.girasol@zonnet.nl;	+31-570-613329
Arvydas APERAVICIUS	TELEBALTIKA	telebaltika@takas.lt;	+370-41-540749
Edmundas ZILINSKAS	SAULES ENERGIJA	saulesenergija@mail.lt;	+370-37-777890
Barry CLIVE	OPTICAL PRODUCTS Ltd	bc@opticalproducts.biz;	+44-20-85204047
Michael David SEELEY	WINSUND	info@winsund.com;	+44-1207-255365
Arthur BADHAM	BADHAM FARMS	badhamfarms@hotmail.com;	+44-1889-564230
Sue EVANS	HEAVENS SOLAR	sue@heavens-solar.com;	+44-1709-579998
Stepas JANUSONIS	MSI	stepas.janusonis@self-formation.lt;	+370-5-2313762
Rüdiger MEYER	ISFH	r.meyer@isfh.de;	+49-5151-999423
Barbara TERHEIDEN	ISFH	b.terheiden@isfh.de;	+49-5151-999413
Stathis TSELEPIS	CRES	stselep@cres.gr;	+30-210-6603369
Henk VAN EKELENBURG	Pro Support	h.van.ekelenburg@prosupport-nl.com;	+31-74-2551160

3.4 Project timetable

3.4.1 Project time-line

In the figure below is the original project planning (taken from the DoW) that was pretty much followed.

Figure 69: Gantt Chart

3.5 Actual versus scheduled manpower and budget spending

The expenditures reflect the partners involvement and material usage. Lower spending than budgetted due to some delay in the delivery of experimental cells, that caused that the field testing didn't take place.

SECTION 4 Other issues

4.1 Benefits to the SMEs

In order to analyse the benefits for the SMEs from the anticipated innovation more in detail an Innovation Impact Assessment has been carried out. Here, the impact of the project on a number of key parameters for processing & quality, marketing & sales, human resources and purchasing has been assessed for each SME participant. The results are shown in Table 12.

Table 12: SME Benefits Assessment

Innovation Impact Assessment **[1 – Minimal; 5 – Very High]**	**MILLENNIUM**	**GIRASOL**	**TELEBALTIKA**	**SAULES ENERGIJA**	**OP**	**WINSUND**	**BADHAM FARMS**	**HEAVENS SOLAR**
Processing & Quality								
Reduced Costs	1	1	1	1	4	1	3	2
Improved Quality	3	3	4	4	4	4	5	4
Improved Environmental Performance	2	2	2	2	3	2	5	3
Reduced Number of Process Steps (reflector)	1	1	1	1	4	1	1	1
Reduced Number of Process Steps (solar cell)	1	1	3	1	1	1	1	1
Reduced Down-time	1	1	5	5	4	5	3	3
Marketing & Sales								
New Business Opportunities	5	5	5	5	5	4	4	3
New Product/Market Combinations	4	4	5	3	5	5	1	3

Increased Customer Loyalty	3	1	2	2	5	2	1	2
Increased Sales (1-3 year)	4	3	5	5	5	5	4	3
Improved Product Safety	1	1	1	1	5	1	5	1
Increased Customer Satisfaction	5	5	5	5	5	5	1	5
Improved Corporate Image	5	5	5	5	5	5	5	5
Human Resources								
Improved Health & Safety	3	1	2	3	3	3	1	1
Improved Employee Satisfaction	2	3	1	2	2	2	3	3
New Knowledge	4	5	5	4	5	4	5	3
Purchasing								
Reduced Dependency on Suppliers	5	2	3	4	5	5	1	2
Reduced Inventories	1	1	1	1	3	1	1	1
Reduced Costs	4	1	1	4	5	4	1	1
Other								
Reduced Probability of Claims	3	1	5	3	5	3	4	1

Annex A - Plan for using and disseminating the knowledge

The Final plan for using and dissemination the knowledge describes schemes for the dissemination of knowledge gained during the project and the plans for promotion of the future project results. This has been an evolving document which was regularly updated by the project partners to give a cumulative overview of the undertaken and planned activities.

The document includes the following three sections:

- Section 1 – Exploitable knowledge and its Use
- Section 2 – Dissemination of knowledge
- Section 3 – Publishable results

SECTION 1 Exploitable knowledge and its Use

1.1 Overview of Exploitable Knowledge

The partners have anticipated co-operation into commercial applications in the future. No problems with the use of existing patents on self-formation technology exist; these will be provided to the project without charge and available after the project for a small royalty (<2% of costprice of the cell). This issue is addressed in the Consortium Agreement.

The scientific work done during first reporting period gave promising results. It is the intention of the Consortium to protect any commercially significant innovations and agreement concerning the protection of knowledge has been made by the partnership. Novel structures and associated manufacturing technologies for bifacial solar cells were developed. The technology has patentability.

Exploitable Knowledge (description)	**Exploitable product(s) or measure(s)**	**Sector(s)** of application	**Timetable** for commercial use	Patents or other **IPR protection**	**Owner** & Other Partner(s) involved
New structure and manufacturing technology for bifacial solar cells	*Bifacial PV cell*	*PV sector*	*2007*	*Patent*	*All partners*
New reflector concept	*Reflector*	*Bifacial cells*	*2008*	*Patent*	***OP**, All SMEPs*

Note: The Reflector is inherently simple, yet sophisticated, and very cheap to manufacture. The optimum reflection surface is determined by optical calculations in this project and can bedescribed by a higher order polynomial function. The SMEs are, however, still reluctant to patent the technology as it may give away more than it protects, and the algorithm itself is not protectable. Also, a slightly adjusted pattern may circumvent the invention. Advice from patent attorneys will be sought as part of the exploiatation plan.

1.2 Exploitable knowledge: item-by-item

Table 13: Exploitable Item #1

Exploitable result	*Description*
Bifacial c-Si PV Cell	New structure and manufacturing technology for bifacial solar cells
Partner(s) involved in exploitation	*Role; activities planned for*
Millennium	Business planning
Telebaltika	Manufacturing of bifacial cells according to new structure
GiraSol	Business planning
OP	Manufacturing of reflector
Other SMEs	To be involved later
Potential exploitation barriers • Technical & Market Entry Barriers • Technical Obstacles • Obsolete policies • New standards • Competitive Actions	Unknown structure may lead that potential customers don't believe the good efficiency is true. They also may be reluctant with respect to long-term performance. The reflector is cheap and provides a self-supporting structure to the PV cells.
Further additional research and development work foreseen after the project	None identified
Intellectual Property Rights protection measures	Patent application in preparation
Commercial activities undertaken • Contacts made • Demonstrations given to potential licensees and/or investors • Comments received (market requirements, market potential, ...);	Some relations have been informed about the project, but in this stage full-scale dissemination of the results is not yet done.
Socio-economic impact	The improved cost/efficiency ratio will make this ORTO-based bifacial solar cells affordable to more people.

SECTION 2 Dissemination of knowledge

2.1 Overview of dissemination activities

Unlike conventional energy systems, photovoltaic applications are often adopted by individuals or non-specialist organisations, whereby price per Watt-peak and system performance reliability are the two key quality elements. Therefore the dissemination of information is one of the most important factors determining the future prospects for PV. The publication of successful experiences with the most mature and professional products is necessary to convince the public and experts about the practicality of the technologies.

REFLECTS promises to reduce the costs of monocrystalline bifacial solar cells. It is however crucial that appropriate and well-targeted information will be provided to targeted groups, emphasizing on the reliability and durability of PV applications. In rural or remote areas it is particularly important to ensure that potential users are aware of PV systems as a sensible alternative to grid extension.

Novel, advanced, bifacial monocrystalline silicon solar cell technology are to be developed with better commercialisation aspects than the standard technology (substantially lower cost/W_p, good possibilities for mass production). A policy of wide dissemination of project results will be pursued in particular focused on potential end users of the project results. Dissemination activities included (or will include):

- Participation in leading conferences related with PV research such as *Eurosun 2006, 21st European Photovoltaic Solar Energy Conference and Exhibition, IX World renewable energy congress, VIP Scientific Forum of the International IPSI-2006 (International Conference on Advances in the Internet, Processing, Systems and Interdisciplinary Research) AMALFI;*
- Disclosure of information through a project brochure (in pdf). The brochure will be compiled to serve as a tool for the dissemination of the project objectives, its status and project results at external events. Pro Support B.V. will be responsible for the production of the brochure. Once the content and format have been agreed by the partners, the pdf version of the brochure will be available on public area of the REFLECTS web site. REFLECTS brochure - containing case studies – will be available as Application Notes to International Associations
- Publications in relevant magazines such as *Photon International, Renewable Energy World* and *PV News*, obviously being careful not to reveal sensitive proprietary information;
- Set-up and maintenance of a project website which is already available on http://reflects.protechnology.lt. REFLECTS web site has been created to provide various information related to the project. It includes a restricted area for the Consortium, mainly used as document repository, and a public section. The site has been opened for public access in March 2005. All the relevant information regarding the REFLECTS web site is to be found in the corresponding Deliverable D8.1 The server is maintained by staff from Pro Support B.V. and is regularly updated. The REFLECTS web site has been created as a main dissemination tool. Not only it presents the goals and objectives of the project in itself,

but it also provides information on its on going activities aiming at the creation of an open discussion within partners.

- Dissemination of information to the networks and established distribution channels of the individual partners. Every partner involved in REFLECTS project is already driven towards promoting the project in its institution. In that perspective, means of dissemination vary: annual review meetings and internal presentations.
- A generic REFLECTS presentation has been developed and follows REFLECTS branding. It can be used by all partners involved in the project to disseminate the project objectives, its status, expected results and can be easily adapted by partners for specific audiences and updated with new information. It currently details the structure of the project in terms of objectives and main results that the project aims to achieve. The presentation aims at attracting interest of research institutes and private companies that are actively involved in PV sector.

In Table 14 below, the dissemination activities have been illustrated.

Table 14: Overview of dissemination activities

Planned / actual Dates	**Type**	**Type of audience**	**Countries addressed**	**Size of audience**	**Partner resp. / involved**
In 2006, Jun	*Eurosun 2006*	Researchers	EU countries	200-250	MSI
In 2006, Aug	IX World renewable energy congress	Researchers, PV manufacturers	All countries	200-300	MSI
In 2006, Sep	21st European Photovoltaic Solar Energy Conference and Exhibition	Researchers, PV manufacturers	EU countries	250-350	MSI
In 2006, Mar	VIP Scientific Forum of the International IPSI-2006 (International Conference on Advances in the Internet, Processing, Systems and Interdisciplinary Research) AMALFI	Researchers	All countries	350-400	MSI
	REFLECTS brochure will be distributed in :				

Planned / actual Dates	**Type**	**Type of audience**	**Countries addressed**	**Size of audience**	**Partner resp. / involved**
Till project closure	British Photovoltaic Association (PV-UK),	European PV manufacturers, researchers	EU countries	200-300	PSU
Till project closure	Austrian PV Association	European PV manufacturers, researchers	EU countries	200-300	PSU
Till project closure	The European Photovoltaic Industry Association (EPIA)	European PV manufacturers, reserachers	EU countries	300-400	PSU
	Publications:				
Till project closure	Photon International	Researchers, general public	To all	-	ISFH, MSI, CRES
Till project closure	Renewable Energy World	Researchers, general public	To all	-	ISFH, MSI, CRES
Till project closure	PV News	Researchers, general public	To all	-	ISFH, MSI, CRES
	Project web-site				
Since June 2005	http://reflects.protechnology.lt	Restricted and public access	To all	-	PSU

SECTION 3 Publishable results

The results achieved by project REFLECTS will be documented in project deliverables. A list of deliverables that have been published during the project is given below (Table 15). Deliverables that have been published have a dissemination level of “public” (PU). It is expected, that these deliverables contain a significant part of the project achievements and therefore dissemination activities will largely base on the results reported in these documents.

A publication have been prepared for 22nd European Photovoltaic Solar Energy Conference.

Table 15: List of Public Deliverables

Deliverable No	ID	Deliverable Title	Delivery Date	Dissemination level
D20	D8.1	Website	6-24	PU
D21	D8.2	Application notes	24	PU
D22	D8.3	Publications	24	PU

3.1 Project LOGO

In order to immediately improve the Project visibility, a logo was designed and will be used in all the dissemination tools, ranking from the web site to fact sheet and brochures:

3.2 REFLECTS Web Site

The first Dissemination task was the creation of a dedicated Web page. The REFLECTS web site (http://reflects.protechnology.lt) has been created in June 2005 to provide various information

related to the project. It includes a restricted area for the Consortium, mainly used as document repository, and a public section.

Information available in **public** section:

- Project summary, which includes short project description and the main project objectives;

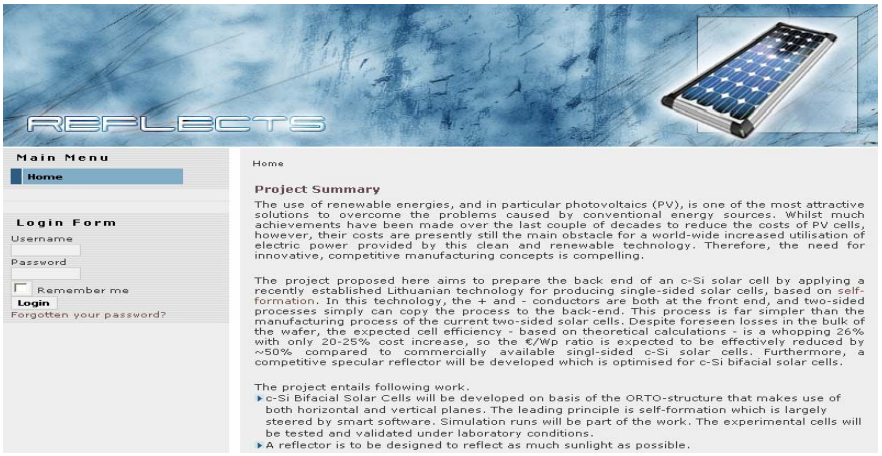

Information available in the **restricted access** area:

- Your profile details. Every partner can check and update his own profile to be available for other project partners.
- Communication. It is available to send a message directly to chosen partner through REFLECTS website.
- Participants. All information about project partners is distributed in this section, including: name of the contact person, telephone number, e-mail address;
- Discussions. This section was created for better communication and dissemination of results between partners;
- Deliverables. This section provides direct access to all project's deliverables with due dates. As the project progresses, links to deliverable documents in a variety of formats are provided;
- Meetings. Information concerning past (Kick-off meeting, 6M meeting and 12M meeting) and future events is available in this section. Partners can download all documents from the meetings including: minutes, power point presentations, photos and oth;

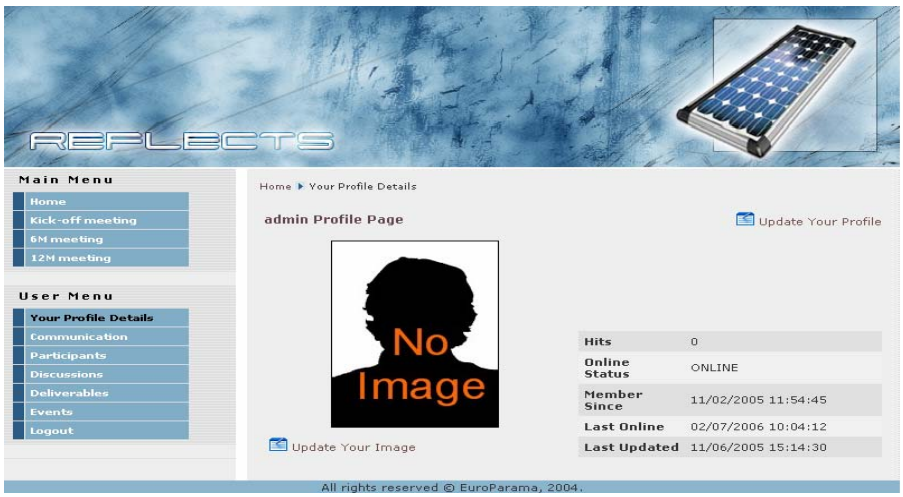

Accessibility

The REFLECTS web site is accessible from any browser working on any platform, since it uses the technologies that should be supported by all browsers. The functionality of the web site was tested on Firefox, Internet Explorer, Netscape, Opera, Mozilla, and LYNX on several platforms, and it worked well in all cases.